Aalto University
School of Chemical
Technology

School of Chemical Technology
Degree Programme of Chemical Technology

Charlotta Johanna Weber

MODELLING AND SIMULATION OF INDUSTRIAL PURGE BINS

Master’s programme in Chemical, Biochemical and Materials Engineering
Major in Chemical Engineering

Master’s thesis for the degree of Master of Science in Technology submitted for inspection, Espoo, 9 January, 2018

Supervisor **Professor Ville Alopaeus**
Instructors **Mohammad Al-Haj Ali, PhD & Juha Visuri, M.Sc. (Tech)**

Aalto University
School of Chemical
Engineering

Aalto University, P.O. BOX 11000, 00076 AALTO
www.aalto.fi

Abstract of master's thesis

Författare Charlotta Johanna Weber

Titel Modellering och Simulering av Avgasningsreaktorer i Industrin

Institution Högskolan för kemiteknik

Professur Kemisk Apparatteknik

Övervakare Professor Ville Alopaeus

Handledare/Granskare Mohammad Al-Haj Ali, PhD och Juha Visuri, M.Sc. (Tech)

Datum 15.11.2017 **Sidantal** 59+4 **Språk** Engelska

Sammandrag
Målet med detta diplomarbete var att få mer utförlig förståelse beträffande avgasningsreaktorer i industrin, vilka används för avgasning av polymerer. Behovet av avgasningen uppstår då industriella polymerer ofta innehåller orenheter i form av flyktiga organiska ämnen (VOC). Dessa härstammar framför allt från kvarblivna monomerer, lösningsmedel eller från sidoreaktioner och är skadliga för miljö och hälsa i stora mängder och bör därför avlägsnas från produkten. Detta kan utföras i avgasningsreaktorer genom att utsätta polymererna för hög temperatur och/eller tryck. Orenheterna avdunstar från polymererna genom diffusion.

I den tillämpade delen härleddes material- och energibalanser för avgasningsreaktorns polymer- och gasfas. Materialutbytet mellan polymer och gasfasen beskrevs genom en balanskoncentration som beskrivs av Henrys lag och den ideala gaslagen. Energiutbytet beskrevs genom direkt parning av de två fasernas energibalanser. Diffusionen genom en enskild polymerpartikel beskrevs genom Ficks lag. En parameter som beskriver fasresistansen för materialutbytet mellan polymererna och gasen tillfogades ekvationerna. Denna beskrivs genom materialutbytes, energiutbytes och diffusionskonstanten. Ekvationerna löstes numeriskt och simulerades i mjukvaran Aspen Custom Modeller (ACM). Experimentell data på materialbalansen fanns tillgänglig från experiment i pilotskala. Data för energibalansen samt evolutionen av koncentrationen i den enskilda polymerpartikeln fanns inte tillgänglig.

Simuleringsresultaten av energibalansen och diffusionen genom den enskilda partikeln gav förväntade resultat. Materialbalansen gav nöjaktiga resultat. Koncentrationen i polymerfasen i den experimentella datan visade en exponentiell förminskning, såsom simuleringen av den enskilda polymerpartikeln. Massbalansmodellen visade även en exponentiell förminskning, men inte en lika drastisk som den experimentella datan. Några förbättringsförslag för modellen inkluderar att göra materialutbyteskonstanten tids- och temperaturberoende för att förstärka kopplingen mellan materialutbyte och tid (eftersom diffusionen är som störst i början av avgasningen) samt materialutbyte och temperatur. Slutligen borde modellen för den enskilda partikeln sammanslås med materialbalansen.

Nyckelord avgasningsreaktor, avgasning, VOCs, materialbalans, energibalans, ACM

Aalto University
School of Chemical
Engineering

Aalto University, P.O. BOX 11000, 00076 AALTO
www.aalto.fi

Abstract of master's thesis

Author Charlotta Johanna Weber

Title of thesis Modelling and Simulation of Industrial Purge Bins

Degree Programme Chemical technology

Major Chemical Engineering

Thesis supervisor Professor Ville Alopaeus

Advisors / Examiners Mohammad Al-Haj Ali, PhD and Juha Visuri, M.Sc. (Tech)

Date 15.11.2017 **Number of pages** 59+4 **Language** English

Abstract

The objective of the master's thesis was to gain a deeper understanding of industrial purge bins, used for de-volatilization of polymers. The deep understanding is needed for optimization of the process and equipment sizing. De-volatilization of industrial polymers is needed since they often contain impurities in the form of volatile organic compounds, which may originate from unreacted monomers, solvents or side reactions. The impurities are harmful for both the environment and health. Besides, it might cause odour and taste when used in different applications; therefore, it should be reduced in the produced polymers. This may be performed through post-production treatment in industrial purge bins, which involves passing liquid or gas (as in this case) at elevated temperatures and/or pressures through some vessel containing the polymer particles (or pellets). The impurities are evaporated and diffused through the polymer.

In the applied part, mass and energy balances were written for the polymer and gas phases of the purge bin. The mass transfer was described through an equilibrium concentration between the phases by Henry's law and the ideal gas law. The energy transfer was modelled through direct coupling of the equations of the phases. The diffusion through a single polymer particle/pellet was modelled by Fick's law. A parameter describing the phase resistance, between the polymer and gas, of the mass and energy transfer needed to be added to each of the above-mentioned equations. These parameters are the mass transfer, energy transfer and diffusion coefficients. The equations were solved numerically and simulated in Aspen Custom Modeller, which offers both a model development environment and flowsheet modelling. Experimental data from pilot scale tests were used for parameter estimation and comparison for the model.

The results of the simulated energy balances and single particle model looked as expected. The single particle model showed an exponential decrease of the impurities in the pellets. Model predictions are close to the experimental data with relative errors that do not exceed 15% in most of the cases studied. The experimental data showed a fast initial decrease of the hydrocarbons. The mass balance model showed similar patterns but less obvious. The mass transfer coefficient should be made time dependent in order to emphasise the exponential decrease and temperature dependent in order to emphasise the temperature effect on the de-volatilization, as an improvement on the model. Finally, the single particle model and the mass balance should be combined, in order to describe the mass transfer through the polymer by Fick's law.

Keywords purge bin, de-volatilization, VOCs, mass balance, energy balance, ACM

PREFACE

This master's thesis was done for the Innovation Centre of Borealis Polymers Oy during the period of June to November 2017.

I thank PhD Johanna Lilja for making it possible for me to write my master's thesis for Borealis Polymers Oy. I would like to thank my advisors at Borealis, PhD Mohammad Al-Haj Ali and M.Sc. Juha Visuri, for their guidance, help and advice during the work. I would also like to thank everyone else at Borealis Polymers Oy who have helped me during the master's thesis, even if they had no obligation to do so. Finally, I would like to thank Professor Ville Alopaeus for the guidance and support through the master's thesis.

I am thankful for having such supportive and encouraging family and friends, who have all supported me through my studies.

Porvoo, January 11th, 2018

Charlotta Johanna Weber

APPENDICIES

APPENDIX 1. The simulation results of mass transfer with a mass transfer coefficient corresponding to the specific grade/run

Abbreviations

VOCs	-	Volatile Organic Compounds
FOGs	-	Semi Volatile Organic Compounds
ACM	-	Aspen Custom Modeller
SWSE	-	Sum of Weighted Squared Errors

1 Introduction

The objective of this master's thesis is to gain a deeper understanding of the operation of industrial purge bins in order to be able to optimize the process and size the equipment. This will be done by modelling and simulating industrial purge bins in continuous and batch modes. Experimental data on pilot scale experiments will be used for parameter estimation and validation of the model.

No or very low levels of impurities in the end product is a desire of every polymer producer. The most common source of impurities are unreacted monomers, oligomers and additives. Other sources are solvents, molecules from side reactions during the production, impurities in the raw material or impurities generated during the downstream process. (1) The impurities considered in this work are hydrocarbons and fall in the category of volatile organic compounds (2). VOCs are harmful for the employers operating the manufacturing processes and even for the end user's. This is seen in the markets sensitivity towards the impurities and the environmental regulations regarding VOCs. (3)

There are some techniques for removing hydrocarbons to be employed during the manufacturing of the polymers but de-volatilization as a downstream process is more commonly used. De-volatilization is a process in which a liquid or gas, as in this case, at elevated temperature is passed through the polymer particles. The elevated temperature lowers the viscosity of the polymers and evaporates the hydrocarbons. This requires diffusion of the hydrocarbons through the polymers. The de-volatilization equipment, i.e. the purge bin, can be designed as continuous, which allows it to be integrated in a continuous manufacturing line. The flow of the gas or liquid can be co-current, cross-current or counter-current. In a batch purge bin, the polymer phase is stationary while the gas or liquid phase is passing through the polymer phase. (4)

The continuous and batch purge bin will be modelled in the sense of mass and energy balances. Also the diffusion in a single particle is modelled. The models are solved numerically and simulated in Aspen Custom Modeller. Experimental data from pilot scale tests are used for parameter estimation and validation of the model. It is investigated whether outliers in the experimental data affect the results of the validation. The effect of the crystallinity in the mass balance is also studied.

2 Impurities in industrial polymers

Polymeric products often contain un-polymerized hydrocarbons, which are enclosed in the polymers. These hydrocarbons are considered as impurities and may originate from unreacted monomers, catalysts, solvents or side reactions during the manufacturing process or after-treatment. Some hydrocarbons are toxic, have an odour and are flammable in large quantities. It is therefore important to reduce the presence of these substances in the product, not only due to environmental regulations but also because of the market sensitivity towards environment and health issues (3). There are a number of patents related to removal of hydrocarbons, which prove the industrial importance of the topic. Several techniques for the reduction of the hydrocarbons exist. The technique to be employed depends on the application of the polymer. However, the removal technique must be planned in such way that the polymer properties remain. (5)

2.1 Sources of hydrocarbons as impurities

The most common source for impurities in industrial polymers is unreacted monomers. This source would be eliminated by leading the conversion to 100%. This is, however, not always possible due to desired polymer properties or the kinetics of the polymerization. Some of the major reasons for low conversion are listed below.

- The cage effect is a scenario in which the radicals/catalysts are trapped in a solvent cage before diffusing apart. This reduces the radical/catalyst efficiency, which reduces the conversion.
- The glass transition temperature of a polymer increases with conversion. If the reaction reaches a conversion, at which the glass transition temperature of the polymer exceeds the reaction temperature, the polymerization stops short and residual monomers are left in the product.
- If the reactivity of co-monomers varies a lot but similar ratios of the two monomers are used, large quantities of one of the monomers remains unreacted.
- De-propagation begins to occur when the reaction temperature of the polymerization reaches the ceiling temperature of the polymer. De-propagation is the reverse reaction to propagation of the polymer chain. (5)

Other sources of impurities may originate from side reactions occurring during the polymerization process, resulting in inert compounds which do not polymerize. The raw materials may contain some non-polymerisable hydrocarbons which eventually end up in the polymer product. Some solvents used in the process may be trapped inside the polymer material during the polymerization or participate in side reactions. Further, impurities may be generated in the post-production treatment of the polymer. (1)

2.2 Volatile Organic Compounds

The hydrocarbons in the polymer often fall in the category of volatile organic compounds (VOCs). These are any compounds with a carbon backbone, which are active in the atmospheric photochemical reactions. Carbon monoxide, carbon dioxide, carbonic acid, metallic carbines and ammonium carbonate are excluded. The International Organization for Standardization (ISO) has defined VOCs as any organic compounds, which has a boiling point less than 260℃ at atmospheric pressure. This would correspond to alkanes between n-pentane and n-heptadecane (n-C5 to n-C17). Formaldehyde and acetaldehyde are also considered as VOCs (6). The classification varies depending on the application of the VOCs containing material. As an example, there are strict standards on this topic in the automotive industry, which are presented in the next section.

Table 1 presents the classification of volatile organic compounds by the world health organisation.

Table 1. Classification of VOCs according to WHO. (2)

Description	Abbreviation	Boiling Point Range [℃]	Example of Compounds
Very volatile organic compounds	VVOC	<0 - 100	propane, butane, methyl chloride
Volatile organic compounds	VOC	50 - 260	formaldehyde, toluene, acetone, ethanol, 2-propanol, hexanal
Semi volatile organic compounds	SVOC or FOG	240-400	Pesticides (DDT), chlordane, plasticizers (phthalates), fire retardants (PCBs, PBB)

There are several motivations for why the VOCs should be removed from polymers. One is that the VOCs are harmful for the health in large quantities. Some symptoms are eye, nose and throat irritation combined with headaches and nausea. Some more severe symptoms are damage to the liver, nervous system and kidney. Further, it has been proven that some VOCs are carcinogenic. The effect of VOCs on the health depends on the level of exposure and length of time exposed. Since many white goods, household equipment, parts of cars and construction materials contain polymeric materials; there is a connection between the VOCs in commercial polymers and indoor air of households, public buildings and transport vehicles (7). Another reason for minimizing the VOCs in polymers is that they play a part in the health of the climate through atmospheric chemistry. The VOCs, which are released to the environment, end up in the atmosphere where oxidation occurs. This has an impact on the greenhouse gases through the reduction of hydroxide, which increases the lifetime of methane in the atmosphere. Aerosols are formed through oxidation of monoterpenes by the VOCs, which have a negative impact on the radiative forcing. (8)

2.3 Analysis methods for VOCs and FOGs

To be able to deliver high quality products to customers, analysis on the impurity content needs to be performed on the end product. It is especially important to have a low content of volatile compounds in the polymeric material used in the interior of cars. The reason for this is that the car is occasionally exposed to high temperatures, which favours desorption of volatile hydrocarbons into a small space (the interior of the car). This results in the smell of a new car which, in fact, means that the air quality in the interior of the car is questionable. There are some standard analyses methods developed specifically to determine the impurity content in polymers used in car applications. (9)

The VDA278 (may be called GMW15634) is a reference method to determine VOCs and FOGs in automotive interior materials, and is used by car manufacturers including Daimler, BMW, Porsche and Volkswagen. This method uses a thermal desorption gas chromatography-mass spectrometry method, which gives the impurity content of non-metallic materials used in the car. The method distinguishes the VOCs, in the range of C1-C25, and the FOGs in the rage of C14-C32. As for the respective response factor, toluene is used for the analysis of VOCs and hexadecane for FOGs. Two analysis are made from

each polymer sample, the VOCs analysis is performed first and the FOGs secondly. The test includes the following procedures. The samples are put into a glass adsorption tube and exposed to hot air flows. The temperature of the air flow is 90 °C for VOCs and 120 °C for FOGs and the time of exposure is 30 minutes for both VOCs and FOGs. The chromatographic separation is performed in Optima5MS column, which is 50 m long, 32 mm in diameter and with a 0,5 µm film thickness. The oven temperature for the FOGs looks as follows. 50 °C for 2 minutes, increased to 160 °C with 25 °C/min and increased to 280 °C with 10 °C/min, which was held for 30 minutes. The VOCs oven temperature looks as follows. 40 °C for 2 minutes, increased to 92 °C with 3 °C/min, increased to 160 °C with 5 °C/min and increased to 280 °C with 10 °C/min, which was held for 10 minutes. (10) A sample placed in a glass adsorption tube is shown in Figure 1.

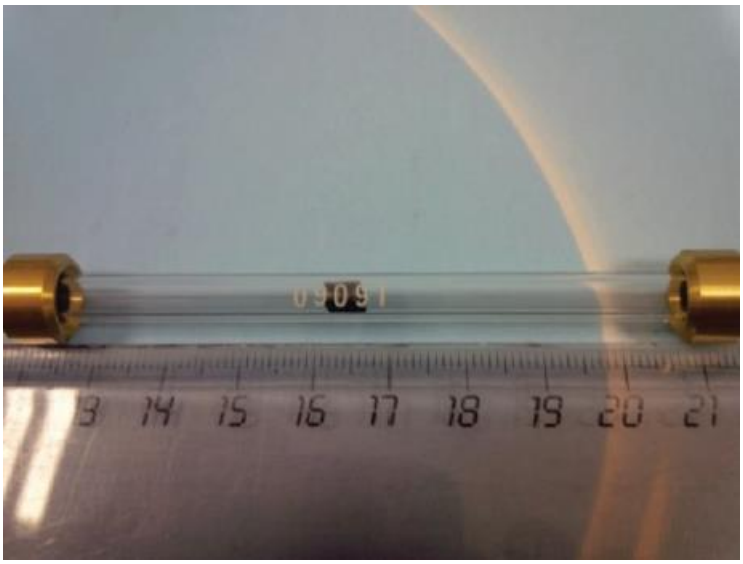

Figure 1. A sample in a glass adsorption tube for the analysis through VDA278. (10)

VDA277 is another reference method for testing the quality of the polymers, used by the automotive industry. The method is based on gas chromatographic analysis, which is performed through head space sampling. The procedure looks as follows. The samples, of 10-25 mg, are sealed in glass flasks and heated at 120 °C for 5 hours. A head space sampler collects 1 ml of the head space after the incubation time. The oven program in the gas chromatogram includes 50 °C for 3 minutes, increasing to 200 °C at a rate of 12 °C/min and stays at 200 °C for 4 minutes. Mainly VOCs are detected through VDA277. (11) The reference for the respective response factor is acetone. Samples placed in the glass flasks are seen in Figure 2.

Figure 2. Samples sealed in glass flasks/headspace vials for the test method VDA277. (11)

3 Examination of the removal of hydrocarbons on a single particle scale

There are a few techniques employed during the manufacturing of the polymers, which prevents the hydrocarbons from accumulating in the final product. If the polymer products, however, contain large amount of hydrocarbons by the end of the production, these need to be removed as a post-production treatment. This requires diffusion of the hydrocarbons through the polymer to the surrounding medium. (4) The diffusion of molecules through polymers varies among different polymer types. The chemical structure of the polymer and the nature of the impurity-molecule determine how volatile the impurity is. The diffusion through the polymers and the interface of the polymer and surrounding media is usually the rate limiting step in the process of removing hydrocarbons. Therefore, the problem needs to be examined on a single particle level, for understanding the preventive actions of eliminating the hydrocarbons in the production of polymers and the diffusion of the impurity-molecules in a post-production treatment. (12)

3.1 Single particle approach for removing hydrocarbons

The single particle approach for removing hydrocarbons from the polymer can be implemented in two different ways. These are preventing the hydrocarbons from accumulating in the polymers in the upstream process and removing the hydrocarbons in the downstream process. In a post-production treatment, already enclosed hydrocarbons are removed from the polymer. As mentioned earlier, it is effective to prevent the hydrocarbons from ending up in the polymer from the beginning. This may be done using different methods during the manufacturing.. Some general techniques for impurity removal are listed below. (4)

- Unreacted monomers can be removed by using several initiators or catalysts, which work in different temperatures, resulting in higher conversions. As an example, the first initiator may work in moderate temperature while the second works in higher. By increasing the temperature, the late initiator can polymerize the remaining monomers.
- The hydrocarbons can be removed from the polymer by letting the polymer solution in contact with an ion exchange resin. Unreacted monomers and other hydrocarbons may be captured from the resin and recycled, if they can be reused in the polymerization.

- The bonds of the organic hydrocarbons can be broken chemically. Smaller hydrocarbons are generally more volatile and diffuse out of the polymer more easily.
- Radiation can be used to reduce the amount of hydrocarbons in the polymer. Microwave, infrared and radio frequency heat the polymer in order to evaporate the VOCs. Ultraviolet and gamma-ray radiation work in a similar way as an extra initiator, in the case of free radical polymerization. (4)

3.2 Mass transfer through the polymer

The transport of molecules in polymers happens through random individual molecular motion. This happens mainly through the void space of the material, which involves sorption, permeation and diffusion. Diffusion is the most significant of these. Looking at diffusion, the driving force is the concentration gradient of the diffusing molecule between the material in the polymer and the bulk phase. Soney et al. describes the fundamentals of the phenomena by Fick's law of diffusion. The diffusion of the penetrant under un-steady state conditions can be described as follows

$$\frac{\partial c}{\partial t} = D\left(\frac{\partial c^2}{\partial r^2}\right) \quad (1)$$

where c is the concentration, t is the time, r is distance of the diffusion and D is the diffusion coefficient. The equation takes the form of equation (2) in the case of spherical coordinates.

$$\frac{\partial c}{\partial t} = \frac{D}{r^2}\left(\frac{\partial}{\partial r}\left(R^2\frac{\partial c}{\partial r}\right)\right) \quad (2)$$

where R is the radius of the polymer particle. (12)

The hydrocarbons move through the void space in the polymer. Some factors affecting the diffusion through the polymer are listed below. The free volume in the polymer and the chain mobility affects the diffusion. The chain mobility describes how the hydrocarbon backbones of the polymer allow movement in relation to each other. There is a connection between increasing chain mobility and improved permeability. Crosslinking decreases the chain mobility since chemical bonds between the polymers chains are formed to make the structure more rigid while the addition of plasticisers improves the chain mobility. Unsaturation in the polymer backbone means greater chain mobility and therefore improved

diffusivity. The diffusion in polymers containing fillers depends on the nature of the filler. Fillers which are permeable increase the diffusion while non-permeable fillers decrease the diffusion. (12)

Looking at the diffusion in different type of polymers, rubbery polymers have the best characteristics, which are unsaturation, segmental mobility and large amount of free volume within the polymer. These all favours the diffusion of hydrocarbons in the polymer. The diffusion in glassy polymers is more complex. The characteristics of glassy polymers are hard and brittle structure with restricted chain mobility. Glassy polymers often have dense structures and little void space. This makes the diffusion in glassy polymers more restricted compared to rubbery ones. The diffusivity in blends depends on the composition. The interaction between the polymers determines the diffusivity in homogenous blends. The interfacial phenomena and the properties of the individual phases determine the diffusivity in heterogeneous blends. (12)

The nature of the penetrating impurity affects the diffusivity. The size and shape of the molecule moving in the polymer influences the rate of diffusion. The diffusion is slower for molecules with longer chain length. The shape of the molecule is crucial, long flat molecules diffuse easier compared to round and bulky molecules. It has been noticed that the shape and size of the penetrating molecules influences the diffusion more in glassy polymers compared to rubbery polymers. (12)

3.2.1 The film theory

The film theory assumes that there is a film at the interface of the mass transfer. In the case of diffusion from the polymer, the film is around the polymer particle as the last barrier for the impurity. The surface concentration, e.g. the concentration in the film, has to be known in order to calculate the mass transfer through the film. The rate of desorption may be calculated according to the following equation.

$$\mathrm{R} = \mathrm{k}(c_{eq} - c) \qquad (3)$$

Here k is a mass transfer coefficient, c_{eq} is the equilibrium concentration and c is the concentration in the bulk phase. The mixing in the bulk phase in assumed to be turbulent so that no variation in the concentration of the bulk phase exists. The mass transfer coefficient adds the phase resistance to the mass transfer. (13)

3.3 Morphology and mass transfer

The structure of the polymer must be known, in order to fully understand the phenomena of removing organic hydrocarbons from polymers. The polymer consists of amorphous and crystalline parts. Additionally, the material can be porous and the pores do not always reach all the way to the surface, which means that they are enclosed inside the polymeric material. Different diffusion coefficients are needed for the different phases. However, Zubov et al. stated that the closed pores can be assumed as amorphous polymer material if the pores are small and there is few of them (14). Additionally, it has to be taken into account that the diffusion is only happening through the amorphous part of the polymer, not the crystalline. A number of articles take the morphology of the polymer into account through the diffusion coefficient. (15)

Vrentas et al. defines the diffusion coefficient, found in equation (1), based on the morphology of the polymer. The free volume theory was used for the non-porous case. The model is based on the idea that the hydrocarbons travel through the free volume, between the chains, of the particle. The diffusion coefficient (D) depends on a pre-exponential constant of D, an overlap factor depending on the amount of free volume shared between different penetrants, the weight fractions of penetrants and polymer, the specific critical hole free volume of the adsorbed hydrocarbons, a parameter defined by the ratio of the previous over the critical free volume of the jumping unit of the polymer chains and the free volume of the system. (16)

It was assumed that the diffusion of the penetrant through the pores happens through a dual mechanism that consists of molecular diffusion through the particle’s pores and the amorphous areas of the polymer. This is illustrated in Figure 3. The diffusion coefficient depends on the collision diameter, molecular weight and pressure of the penetrant, the Leonard-Jones potential, temperature and energy of the interaction of the penetrating molecules. (16) The Leonard-Jones potential is a mathematical model which describes the interaction between molecules (17). The diffusion through the amorphous media depends on the temperature, degree of crystallinity and number of diffusing molecules. The overall diffusion coefficient is a combination of the porous and amorphous diffusion coefficient. (16)

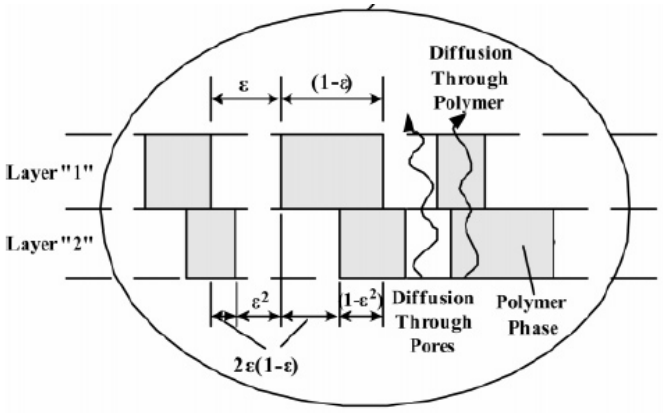

Figure 3. Illustration of the diffusion of hydrocarbons through pores and amorphous polymeric material (18).

Seda et al. found that the pores in the polymer particle have an effect on the diffusivity only in polymers with porosity larger than 8%. Further, it was stated that the dynamics of the degassing cannot be described only by Fick's law. The reason is that the characteristic diffusion length has to be taken into account. This means that the morphology in terms of porosity (larger than 8%) and crystallinity strongly affects the transport of gases inside the polymer. (15)

Bobak et al. assumes that the polymer consist of compact granules embedded in the polymeric material, which all have a catalyst particle in the centre. The granules inside the polymer were divided into two sizes, small and large. This gives two different radii for the granules, which are significantly smaller than the radius of the polymer particle. This is seen in Figure 4. (19)

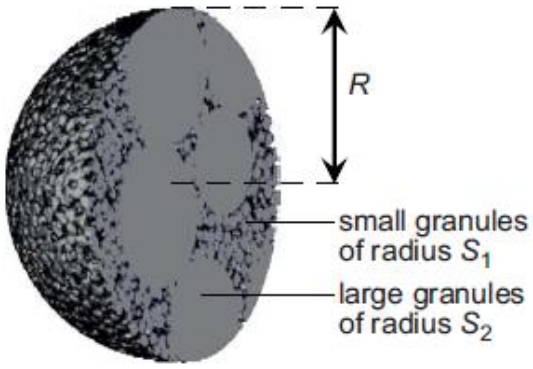

Figure 4. Polymer particle containing granules of smaller and larger sizes. (19).

Individual mass transfer equations, based on Fick's law, were modelled for the two granule sizes. A mass balance equation was derived for the pores in the polymer, in which penetrants from the granules enter the pores and then leave the pores through diffusion to the bulk phase. The concentration in the pores depends on the porosity. The transport of the penetrant in the pores can be described by Fick's law, by Darcy's permeation or by a combination of these two. Darcy's permeation describes the flow of a liquid in a porous media through the viscosity of the fluid and the pressure drop over a distance (20). (19)

4 Removal of hydrocarbons in industrial purge bins

The post-production treatment of polymer pellets, for removing hydrocarbons as impurities, has become more common. Numerous methods have been studied and many patents exist in this area. When the chemical structure of the polymer and the nature of the impurity-molecule are known, the de-volatilization process needs to be planned in such way that most hydrocarbons are removed. (4)

4.1 Purging

Purging always requires penetration of the hydrocarbon through the polymers. This is usually performed in the downstream process in a purging vessel. Some post-production treatment methods are listed below.

- The process of exposing the polymer to high temperatures and/or high pressures is called de-volatilization. This is explained more detailed in the next section.
- Spray-drying involves spraying the melted product at a temperature above the boiling point of the hydrocarbons. Through this, the surface of the polymer particles is significantly decreased which favours the diffusion of the hydrocarbons.
- In supercritical extraction, an extraction media is compressed at elevated pressures before it is led into contact with the polymer. When the extraction media is expanded in atmospheric pressure, the polymer is swollen and the free volume inside the polymer is increased. The final stage in the process involves de-pressurizing the polymers, when the hydrocarbons diffuse out of the polymer along with the supercritical fluid.
- In stripping, gas or steam is purged through an emulsion containing the polymer. The hydrocarbons travel from the polymer through the liquid phase to the gas phase. The mass transfer is, in some cases, more effective in this set up, when comparing stripping to de-volatilization.

4.2 De-volatilization

The most common technique for removing hydrocarbons from polymers is through de-volatilization by extraction. In this technique, the hydrocarbons are separated from the polymeric material to another media (extraction media), which is passing through the polymeric material. In this way, the hydrocarbons are physically diffusing through the polymer to the extraction media. This is also called purging. Different extraction media (also

called stripping agents) have been used. BASF uses hot water, there is an U.S. patent describing the use of supercritical propylene and experiments with methanol have been successful. (21) The most common extraction medias are, however, steam, air and nitrogen gas. The extraction process can be co-current, counter-current or cross-current. The counter-current extraction has shown the best results. (4)

There is a variety of equipment used for de-volatilization of polymers. The de-volatilization process can be operated batch wise or continuously in equipment, which allows the extraction media to pass through the polymeric material. The continuous process is popular since this can be implemented as a part of a continuous manufacturing line of polymers and, as mentioned earlier, is the most effective alternative of operation. (4)

The effectiveness of the de-volatilization can be improved through simple design changes. As an example, mixing can be added to the process in order to renew the polymer-extraction media interface. The performance of the de-volatilization equipment is improved by increasing the temperature, since the hydrocarbons are more volatile in higher temperatures. Also, the viscosity of the polymer is lowered in higher temperatures, which makes the polymer softer, which allows the hydrocarbons to move inside the polymer more easily. Another way to improve the performance is by lowering the pressure to a value lower than the partial pressure of the hydrocarbons in the bulk gas, which makes the hydrocarbons diffuse faster through the polymer. This is seen in the film theory in section 3.2.1, since the driving force of the mass transfer is the difference between concentration of the hydrocarbon in the bulk phase and at the surface of the polymer. This can be done by having a continuous extraction media flow through the polymers.

The size and shape of the polymer particle is critical for the de-volatilization. The diffusion path is shorter and the polymer-stripping agent interface is larger, since the surface to volume ratio is increased, with smaller particles. As mentioned in section 3.3 by Seda et al., the diffusion length is critical for the de-volatilization. The diffusion length is strongly connected to the shape and size of the particle. (4)

4.2.1 Henry's law

The amount of hydrocarbons in the bulk phase during the de-volatilization/stripping can be estimated by Henry's law. The law states that the amount of dissolved gas, in a liquid or solid phase, is proportional to the partial pressure of the same component in the gas phase.

A proportional factor called Henry's law constant is needed for the relation, which is seen in equation (4). (22)

$$H = \frac{c_p}{p} \quad (4)$$

where H is the henrys law constant, c_p is the concentration of the component in the liquid/solid and p is the partial pressure in the gas phase. Henrys law can be used when modelling the relation between the concentration of hydrocarbons in polymers and the surrounding media. This has been stated by Seda et al., Zubov et al., Guitara el al. and Colyan et al. (14) (15) (23) (24). A number of tables on Henry's law constant for hydrocarbon exist. The constant is temperature and pressure dependent and has to be selected carefully. (22)

4.3 Design of de-volatilization equipment

As already mentioned, counter-current extraction has proven to be the most effective in terms of de-volatilization. This means that the extraction media is moving in the opposite direction from the polymers. It is favourable to use the gravitation for the motion of the polymer particles, meaning that the purge bin is vertical and the polymers flow downwards as the gas flows upwards. (3) A schematic figure of a counter-current packed bed is seen below.

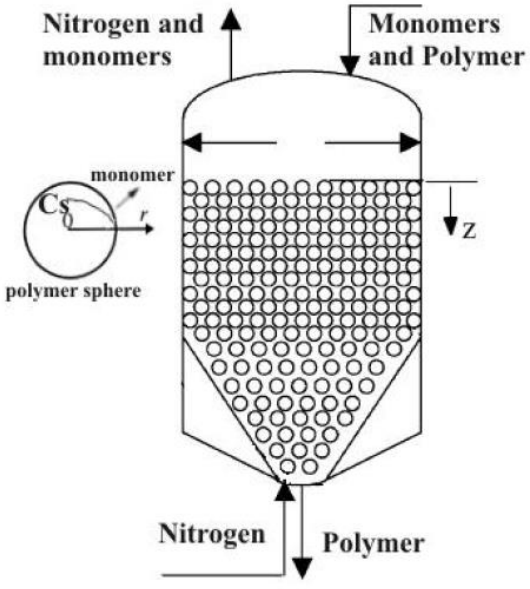

Figure 5. A schematic figure of a packed bed (24).

A well designed purge bin gives a uniform distribution of polymers, after the treatment. This means that the post-treatment concentration of the VOCs is near equal in the polymer particles. This is achieved by having a uniform flow of gas and polymer particles. Velocity differences of the particles gives different residence times in the equipment and therefore different concentration profiles in the end product. Usually the size and density is assumed to be constant for all polymer particles, when planning and modelling the equipment. There are, however, small differences in the shape and density of the polymer particles in real life. This has to be taken into account since the motions of the particles has to be uniform. Some issues, which may occur during the de-volatilization, are listed below.

- Arching or bridging, in which the particles are caked at the outlet of the equipment, should be avoided by planning the angle of the walls and size of the outlet.
- The risk of cross-contamination may occur if the equipment is poorly sized. In this case, the hydrocarbons are transferred between particles through the extraction media.
- Flooding is a scenario where the flow of the particles is uncontrolled and non-uniform. In other words, there are areas that moves faster through the equipment compared to the surrounding area.

The above-mentioned problems occur because the funnel flow pattern is disturbed. This can be avoided by careful planning of the angle of the walls and keeping the friction of the walls in mind. The particles have to pass the wall of the vessel smoothly and thus the friction of the wall material has to be moderate. (25) The inlet gas steam, e.g. the extraction media, has to be flowing without disturbing the flow of the polymers but still reaching all of them. (26)

The optimal dimension of the equipment gives the polymers a residence time in which the hydrocarbons are aerated to a desired value. However, it is unfeasible to have equipment in which the polymers are still being purged after the hydrocarbons have diffused. Figure 6 represents some simulated scenarios of de-volatilization from the industry. (26)

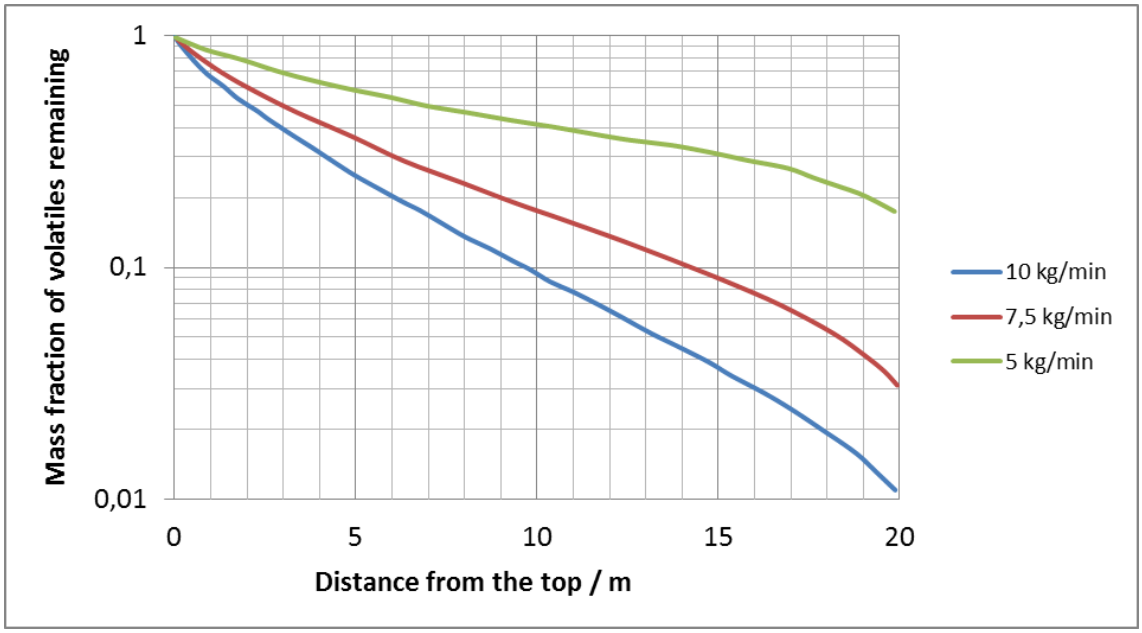

Figure 6.The evolution of the volatiles concentration in the pellets as a function of the height of the equipment. (26)

The figure represents the amount of volatiles remaining in the polymer as a function of the distance from the top of the equipment. The extraction media is air in this case. As it is seen in the figure, three different gas mass flow rates have been tested, in order to reach the desired final mass fraction of 0,03. Comparing the different gas flow rates, 7,5 kg/min provides a feasible solution. The residence time would have to be increased, for the 5 kg/min, by increasing the height or diameter of the equipment, if the conditions remain the same for the 5 kg/min scenario. The outcome of the 10 kg/min process is less than 0,03 but it is not necessary to continue the purging after the desired mass fraction is reached. If the purging conditions remain the same, the diameter or height could be decreased. In this way energy and time is saved. (26)

5 Modelling of purge bins

A mass balance and energy balance needs to be modelled, in order to simulate the dynamics of the purge bin. The model should provide a good representation of the physical system. However, it is impractical to have a complex model and therefore the simplest representation, which gives feasible results, should be chosen.

5.1 Mass balance

The following section presents three different approaches for modelling the mass balance for an industrial purge bin.

Cozewith examined the removal of solvent from spherical particles with the intention to be able to optimize the process for removing residual solvents molecules from polymer particles. Fick's law of diffusion was used to model the diffusion in the polymer pellets. The diffusion coefficient was assumed as an integral average over the concentration profile of the solvent. An equation describing the concentration of solvent in the particle as a function of time was derived. Only the diffusion through the polymeric material was modelled, not considering the material balance at the interface and outside the pellet. This results in equation (5), which is an integral over the residence time distribution function and the weight fraction of solvent in a particle, which gives the average weight fraction of the hydrocarbons in the particles in the particle-bulk media slurry at a specific time. (27)

$$\overline{\mathrm{X}} = \int_0^\infty \mathrm{XE(t)dt} \qquad (5)$$

Where $\overline{\mathrm{X}}$ is the average weight fraction of VOCs in the particle, X is the weight fraction of solvent in the particle and $\mathrm{E(t)}$ is a function describing the residence time based on the number of tanks in series. (27)

Chen et al. developed a mathematical model for extraction of oligomers, from spherical polymer pellets, with the help of a solvent. The model may be used for batch or continuous processes. The hydrocarbons diffuse linearly from the interior of the polymer pellet to the outer surface, the hydrocarbons are transferred to the bulk phase at the interphase of the pellet by diffusing through a stationary film (described in section 3.2.1) around the pellet and macroscopic movement in the form of convection and dispersion of the hydrocarbons takes place in the bulk phase. Fick's law of diffusion is used to model the diffusion through the

polymer. Two mass balance equations were derived for the macroscopic model, based on the microscopic equations. One for the evolution of the concentration of the penetrant in the pellet and one for the bulk phase. A term explaining the axial dispersion and a term explaining the convective evolution of the concentration of the hydrocarbons is present in the mass balance for both phases (the first and second term on the left hand side). The desorption rate of the hydrocarbon, in the form of Fick's law of diffusion, is added to the polymer phase mass balance. The gas phase contains additionally a term explaining the mass transfer of hydrocarbons from the polymer to the gas phase. Three dimensions were used when modelling the full system, the radius of the pellet, the axial position in the column and the time. The extraction profiles were successfully compared to experimental values. The equations are seen below (3)

$$0 = \frac{1}{\mathrm{Bo_p}}\frac{\partial^2 c_p(\mathrm{x,r})}{\partial \mathrm{x}^2} - \frac{\partial \mathrm{c_{p,f}(x,r)}}{\partial \mathrm{x}} + \frac{\sigma}{r^2}\frac{\partial}{\partial r}\left[r^2\frac{\partial c_p(x,r)}{\partial r}\right] \quad (6)$$

$$0 = \frac{1}{\mathrm{Bo_g}}\frac{\partial^2 c_g(\mathrm{x})}{\partial \mathrm{x}^2} - \frac{\partial c_g(\mathrm{x})}{\partial \mathrm{x}} - 3\eta\gamma\rho(c_g(\mathrm{x}) - \mathrm{H[u(x,1)]}) \quad (7)$$

where Bo is the Bondenstein number, which depends on the flow velocity of the phases, the reactor length and the dispersion coefficient. c is the concentration of the impurity and sub index g is for the gas and p for the polymer. r is the radial coordinate and x is the axial coordinate. η is the phase ratio, γ is the phase resistance number, ρ the density, $\mathrm{H[u(x,1)]}$ is the dimensionless distribution function and the sub index f stands for the feed. (3)

The model was compared to experimental data with good results. It is proposed that the addition of an adsorption term would improve the model. In this way, the mass transfer from the gas to the polymer is taken into account. (3)

Guarita et al. modelled and simulated the process of stripping hydrocarbons from linear low-density polyethylene. Fick's law of diffusion was used to model the diffusion through the polymer. The free volume theory described by Kanellopolous et al. was used to describe the diffusion coefficient. A counter-current moving bed system mass balance was modelled for the polymer phase including a convective term, the VOC mass transfer term and an axial distribution term. The mass balance for the gas phase includes a convective term, a term describing the axial change in the velocity of the gas and a mass transfer term. Equation (8) and (9) show the mass balances in the polymer and gas phases respectively. (24)

$$\frac{\partial c_p}{\partial t} + v_p \frac{\partial c_p}{\partial x} = \frac{1}{r^2}\frac{\partial}{\partial r}(r^2 q_s) + D_b \frac{\partial^2 c_p}{\partial x^2} \quad (8)$$

$$\varepsilon \frac{\partial c_g}{\partial t} + v_g \varepsilon \frac{\partial c_g}{\partial x} + c_g \varepsilon \frac{\partial v_g}{\partial x} = -\rho_s s q_s \quad (9)$$

where the subscript p stands for solid and g for gas. t is time, c is concentration, x is the axial coordinate, r is the radial coordinate of the particle, ρ is the density, s_v is the mass transfer area per column volume, v is the superficial velocity, ε is the porosity and D_b is the axial distribution coefficient. The term q_s describes the desorption rate of the hydrocarbon and is defined through equation (10).

$$q_s = \sum_{j=1}^{n} D \frac{\partial c_p}{\partial r} \quad (10)$$

where D is the diffusion coefficient. (24)

The model was compared to experimental data, showing higher VOC values than the experimental data. The error between the numerical and experimental results was lowered by adjusting the diffusion coefficient. (24)

Among the above-mentioned approaches, the one from Cozewith is the simplest; while the one from Chen et al. is the most advanced. The approach from Guitara et al. is, however, similar to the one from Chen et al, with few differences. Chen et al. takes the phase resistance and the distribution of volatiles between the phases into account. Guitara et al. takes the change in velocity, as a function of the axial coordinate of the equipment, into account.

5.2 Energy balance

The following section presents two different approaches for modelling the energy balance of industrial purge bins.

Guitara et al. derived an energy balance for the process described in section 5.1. The heat capacity together with the specific mass was used to describe the change in energy with respect to time and the axial coordinate of the equipment in both the polymer and gas phase. For the polymer phase, the mass transfer between the polymer and the gas and the heat for vaporization of the hydrocarbons were added. The heat transfer between the polymer and

gas was also added in the energy balance for the gas, together with the heat transfer between the gas and the purging vessel walls. The equations are seen below.

$$(1-\varepsilon)\rho_p c_{pp}\frac{\partial T_p}{\partial t}+(1-\varepsilon)v_p\rho_p c_{pp}\frac{\partial T_p}{\partial x}=h_p s_v\left(T-T_p\right)+\sum_{j=1}^{n}\Delta H_p s_v q_p \qquad (11)$$

$$\varepsilon\rho_g c_{pg}\frac{\partial T_g}{\partial t}+\varepsilon v_g\rho_g c_{pg}\frac{\partial T_g}{\partial x}=h_p a_v(T_s-T)+h_w s_w(T_w-T) \qquad (12)$$

The subscript g stands for gas, p for polymer, v for gas-to-polymer, w for gas-to-wall and j for a specific hydrocarbon. ε is the porosity, ρ is the specific mass, c_p is the heat capacity, T is the temperature, h is the heat transfer coefficient, s_v is the heat transfer area per column volume, ΔH is the heat of vaporization, h_p is the gas-solid transfer coefficient, q is the desorption rate and z is the axial coordinate.

Hänchen et al. derived an energy balance for a packed bed of magnesium silicate rocks. The solids are stationary while the extraction media is moving in this example. The model considers convection and conduction of the heat while the following assumptions were made: 1D Newtonian flow, uniformly packed bed with constant heat capacity, uniform temperature of the particles, no internal heat generation, no mass transfer, radiation heat transfer and heat conduction in the fluid phase are neglected. The equations look as follows. (28)

$$\frac{\partial T_g}{\partial t}+\frac{G}{\rho_g^{\varepsilon}}\frac{\partial T_g}{\partial x}=\frac{h_v}{\rho_g c_g^{\varepsilon}}\left(T_s-T_g\right)+\frac{h_w D\pi}{\rho_g c_g A\varepsilon}\left(T_{inf}-T_g\right) \qquad (13)$$

$$\frac{\partial T_s}{\partial t}=\frac{h_v}{\rho_s c_s(1-\varepsilon)}\left(T_g-T_s\right)+\frac{k_{s,eff}}{\rho_s c_s(1-\varepsilon)}\frac{\partial^2 T}{\partial x^2} \qquad (14)$$

where the sub-indexes s is solid and g is gas. T_{inf} is the ambient temperature, T temperature, t time, ρ density, ε void fraction, x the axial coordinate, c specific heat capacity, A area of bed cross section, h_w heat transfer coefficient through the wall, G mass flow per unit cross section, D tank diameter, h_v volumetric heat transfer coefficient between fluid and particle and $k_{s,eff}$ the thermal conductivity of the solid. (28)

Comparing the previous (equations (11) and (12)) to the later energy balances (equations (13) and (14)) both contain convective terms and a term describing the energy transfer between the gas and solids. Further, the gas energy balances contain a term describing the energy transfer between the wall and the gas. A big difference between the cases, however, is that the later one contains a convective term for the solid phase even if it is stationary. If

the previous case would be modelled with a stationary solid phase, v_p would be zero and the convective term would be eliminated. Another visible difference is the term describing the heat of vaporization of the hydrocarbons in the previous case. This is not present in the latter case.

5.3 Discretization methods

The problem, described in section 5.1 and 5.2, consists of parabolic partial differential equations, of second order. In order to solve the equations numerically, they must be discretized. The grid-method or finite-differences method is the most common for discretization (29). A grid is used to divide the body/area under consideration into pieces of finite area or volume. An example of this grid is seen in Figure 7.

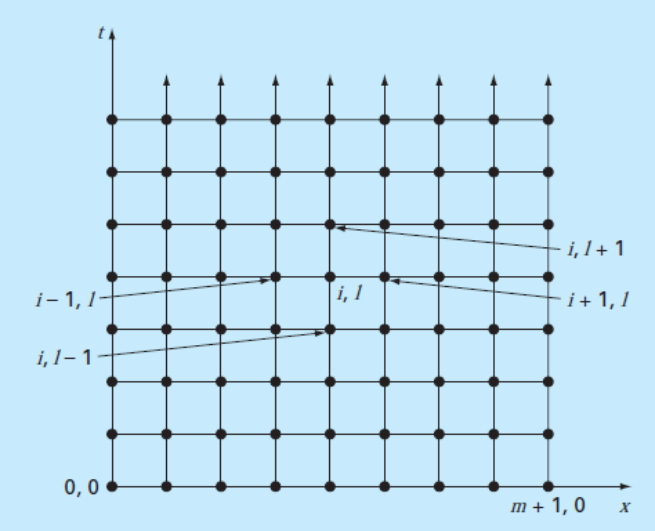

Figure 7. Grid used for the finite-differences discretization method. (30)

In this case, only the radial/axial direction is discretized, which means that only the x-direction in the figure is examined and not the t-direction. Mainly three different approaches are used in the discretization: central, forward and backward. Looking at equation (2), the discretized equation by central finite-differences is found in equation (15).

$$\frac{\partial c_p}{\partial t} = \frac{2D}{D}\frac{c_{i-1}-c_{i+1}}{2dr} + D\frac{c_{i-1}-2c_i+c_{i+1}}{dr^2} \qquad (15)$$

The discretized equation using forward finite-differences is found in equation (16).

$$\frac{\partial c_p}{\partial t} = \frac{2D}{r}\frac{c_{i+1}-c_i}{dr} + D\frac{c_{i+2}-2c_{i+1}+c_i}{dr^2} \qquad (16)$$

The discretized equation using backward finite-differences is found in equation (17).

$$\frac{\partial c_p}{\partial t} = \frac{2D}{r}\frac{c_i - c_{i-1}}{dr} + D\frac{c_i - 2c_{i-1} + c_{i-2}}{dr^2} \quad (17)$$

When the flow of the two phases, e.g. gas and polymer, is the opposite in a counter current purge bin, both the forward and backward difference is needed in the discretization. (30)

APPLIED PART

6 Model development

The de-volatilization in a purge bin was modelled in a continuous and batch mode. A schematic picture of the continuous purge bin is seen in Figure 8 and the batch purge bin is seen in Figure 9.

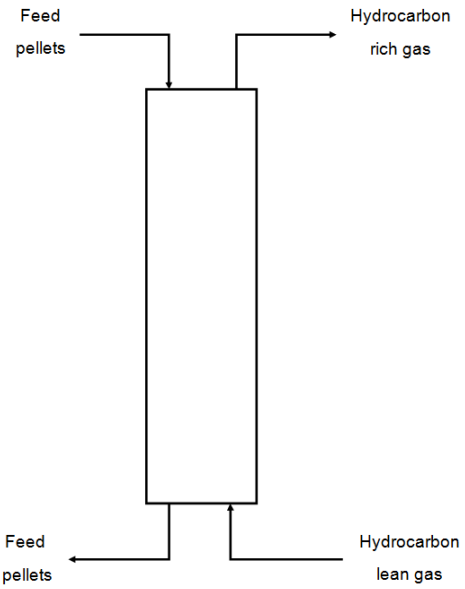

Figure 8. Schematic figure of the continuous purge bin.

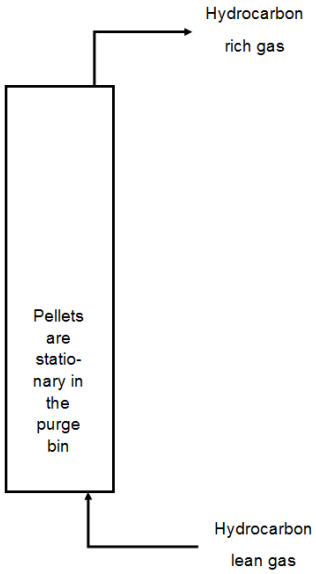

Figure 9. Schematic figure of the batch purge bin.

The following assumptions were made.

1. The polymer pellets are spherical and of the same radius
2. The porosity of the bed is constant
3. The polymer density is constant, which means no swelling
4. There is no or very small pressure drop over the vessel
5. Mass transfer limitations of hydrocarbons are due to a gas film around the particle and thermodynamic equilibrium
6. No chemical reactions occur
7. No back mixing occur
8. The temperature and concentration is constant in the radial direction of the vessel of both the polymer and gas phase
9. The heat of evaporation of the hydrocarbons is neglected, since the concentration of these are small
10. There is no energy transfer between the system and surroundings, except the air and gas flows at the inlet/outlet

6.1 Continuous process equations

A mass balance equation, equation (18), for the VOCs was modelled for the gas phase. The first term on the right hand side of the equation is the convective term, which described the hydrocarbons entering and leaving the control volume with the media (gas in this case). The second term describes the amount of hydrocarbons diffusing from the polymer to the gas. It was assumed that the diffusion happens only in the amorphous part of the polymer and therefore the term (1-y), describing the amorphous part of the polymer, is present in the mass transfer.

$$\varepsilon\frac{\partial c_g}{\partial t} = -\varepsilon v_g\frac{\partial c_g}{\partial x} - (1-y)ks_v(c_g - c_{eq}) \qquad (18)$$

Initial condition: $c_g = 0 \text{ at } t = 0$

Boundary conditions: $c_g = c_{g,out} \text{ at } x = h,\ c_g = c_{g,in} \text{ at } x = 0$

Ɛ is the porosity, c_g is the hydrocarbons concentration in the gas, t is time, v_g is the superficial gas velocity, x is the axial coordinate, y is the crystallinity, k is the mass transfer coefficient,

s_v is the surface to volume ratio, h is the height of the purge bin and c_{eq} is the equilibrium concentration.

Volatile hydrocarbons mass balance in the polymer phase is described by equation (19). Here the sign for the second term on the right had side is opposite compared to the gas phase equation, since the hydrocarbons are moving in an opposite direction. Also the sign of the convective term is the opposite, since the convection is happening in an opposite direction due to the fact that the purge bin is counter-current.

$$(1-\varepsilon)\frac{\partial c_p}{\partial t} = (1-\varepsilon)v_p\frac{\partial c_p}{\partial x} + (1-y)ks_v(c_g - c_{eq}) \quad (19)$$

Initial condition: $c_p = c_{p,in}\ \text{at}\ t = 0$

Boundary conditions: $c_p = c_{p,out}\ \text{at}\ x = h,\ \ c_p = c_{p,in}\ \text{at}\ x = 0$

c_p is the hydrocarbon concentration in the polymer and v_p is the superficial polymer velocity.

The diffusion inside the polymer particle, as a function of the radius, is described through equation (20). This is an equation based on Fick's law of diffusion with spherical coordinates, as described in section 3.2. As boundary conditions, it is assumed that no diffusion is happening over the centre of the polymer and the concentration at the outer surface of the polymer is the same as the equilibrium concentration at the polymer phase of the film.

$$\frac{\partial c_{sp}}{\partial t} = \frac{2D}{rad}\frac{\partial c_{sp}}{\partial r} + D\frac{\partial^2 c_{sp}}{\partial r^2} \quad (20)$$

Initial condition: $c_p = c_{p,in}\ \text{at}\ t = 0$

Boundary conditions: $c_p = c_{p,eq,p}\ \text{at}\ r = rad,\ \ \frac{\partial c_p}{\partial r} = 0\ \text{at}\ r = 0$

c_{sp} is the concentration in a single pellet, rad is the radius of the polymer, r the radial position in the pellet and D is the diffusion coefficient.

The equilibrium concentration at the surface of the pellet is determined through Henry's law, see equation (21). The partial pressure of the hydrocarbons is determined by the ideal gas law, equation (22).

$$p_g = c_p H \quad (21)$$

$$p_g = c_{eq} R T_g \quad (22)$$

Where P_g is the partial pressure of the hydrocarbon in the gas phase, H is Henry's constant, R is the ideal gas constant and T_g is the temperature of the gas.

The energy balance for the gas phase was derived as follows. The change in temperature over time depends on the amount of energy entering and leaving the control volume (the convective term) and the amount of energy transferred between the gas and polymer phase in the control volume. This is seen in equation (23).

$$\varepsilon \rho_g C_{pg} \frac{\partial T_g}{\partial t} = \varepsilon v_g \rho_g C_{pg} \frac{\partial T_g}{\partial x} - h_p s_v (T_p - T_g) \quad (23)$$

Initial condition: $T_g = T_{g,0}$ at $t = 0$

Boundary conditions: $T_g = T_{g,out}$ at $x = h$, $T_g = T_{g,in}$ at $x = 0$

ρ_g is the density of the gas, c_{pg} is the specific heat capacity of the gas, h_p is the heat transfer coefficient and T_p is the temperature of the polymer.

The energy balance for the polymer phase looks similar as for the gas phase. The direction of the heat transfer between the polymer and gas face is the opposite as well as the direction of the convective term. This is due to the same reasons as the ones explained for the mass balance. The term describing the heat of vaporisation, see equation (11), is not included since the concentrations of the hydrocarbons are very small; thus, the term is negligible as can be depicted in Equation (24).

$$(1 - \varepsilon) \rho_p C_{pp} \frac{\partial T_p}{\partial t} = -(1 - \varepsilon) v_p \rho_p C_{pp} \frac{\partial T_p}{\partial x} + h_p s_v (T_p - T_g) \quad (24)$$

Initial condition: $T_p = T_{p,0}$ at $t = 0$

Boundary conditions: $T_p = T_{p,out}$ at $x = h$, $T_p = T_{p,in}$ at $x = 0$

ρ_p is the density of the polymer and C_{pp} is the specific heat capacity of the polymer.

6.2 Batch process equations

The mass balance equation for the gas phase in the batch process looks the same as in the case for the continuous process, equation (18). The mass balance equation for the polymer

phase is seen in equation (26). The equation differs from the continuous process in the sense that there is no convective term present, since the polymer phase is stationary.

$$(1-\varepsilon)\frac{\partial c_p}{\partial t} = (1-y)k s_v (c_g - c_{eq}) \quad (26)$$

Initial condition: $c_p = c_{p,in}$ at $t = 0$

The equation for the diffusion inside the particle is the same as for the case of a continuous process. The same stands for the calculation for the equilibrium concentration through Henry's law and the ideal gas law, seen in equation (21) and (22).

The energy balance for the gas phase is the same as in the continuous case and is seen in equation (23). As in the case of the mass balance, the convective term is not present in the energy balance of the polymer phase. This is because the polymer phase is stationary and therefore there is no convection in the axial direction. The energy balance of the polymer phase is seen in equation (27).

$$(1-\varepsilon)\rho_g c_{pg}\frac{\partial T_g}{\partial t} = h_p s_v (T_p - T_g) \quad (27)$$

Initial condition: $T_p = T_{p,0}$ at $t = 0$

7 Simulation

Since the variables in the equations (18)-(27) are dynamic and coupled, they form a dynamic system of partial differential equations. A numerical solution would be complicated without using any simulation software, since much iteration would be needed. Therefore, Aspen Custom Modeller (ACM) was used for the simulation.

7.1 Aspen Custom Modeller

Aspen Technology offers software for process simulation. The software allows for better understanding of the process, optimization, equipment planning, economic evaluation, supply chain planning, process control design and risk & performance management. The ACM offers both a model development environment and complete flow sheet modelling. The flow sheet allows for blocks which represent a part of the process, e.g. a reactor or separation equipment, connected through streams. The performance of the blocks can be described through ACM, where users can program custom made process models through a code written in a specific format. Some of the main abilities of ACM are listed below.

- Interface to C++, C or FORTRAN legacy modes
- The ability to be exported to Excel or other Aspen programs
- Features/solvers for numerical solutions of ordinary differential and partial differential equations
- Dynamic and steady state simulation modes
- Estimation and optimization tools
- Pre-configured tables and forms for entering input data or reviewing results
- The ability to create libraries of custom models
- Integration with Aspen Polymer Plus for modelling polymer processes
- Possibility of using Aspen databases for thermodynamic, physical and chemical properties of the model components

7.2 Continuous steady state simulation

The continuous operation of the purge bin was simulated as a steady-state simulation. The reason for this is that the time dependency of de-volatilization of the hydrocarbons is described by the residence time which depends on the velocity of the polymer, the dimensions of the purge bin and density of the polymer. Therefor the axial position in the equipment is a function of time.

Equations (18), (19) and (21)-(24) were used for the simulation of the steady state solution. Equation (20) was excluded which means that the diffusion as a function of the radius in the pellet was neglected at this point. Instead, it was assumed that the concentration is uniform in the pellet and the equilibrium concentration is a function of the concentration in the pellet. The equilibrium concentration was calculated through equation (21) and (22). The partial differential equations were discretized as explained in section 5.3. Since the flow of the polymer and gas is the opposite in the vessel, different discretization methods were used for the two phases. The backward finite-differences method was used for the flow of the gas and forward finite-differences for the polymer, according to equation (16) and (17). Looking at the boundary conditions of equations (18) and (19), only the boundary conditions of the inlets were defined while the outlets were calculated. Further, initial conditions were defined.

The energy balance was simulated through equations (23) and (24). As for the mass balances, the equations were discretised as in section 5.3 and the forward finite-difference was used for the polymer phase while the backward finite-difference was used for the gas phase. As in the previous case, the boundary conditions were applied on the inlet while the outlet properties were estimated through the equations. Initial conditions were defined.

7.3 Batch dynamic simulation

The batch operation of the purge bin was simulated dynamically. Since the polymer phase is stationary and the gas flow rate is significantly larger than the rate of the mass transfer, it was assumed that there is no or very small concentration gradient in the axial direction of the purge bin and thus is the concentration change only time dependent, not a function of the axial coordinate as in the continuous case. The concentration of the gas changes with the axial coordinate of the system, since the phase is not stationary and therefore contains a convective term.

Equations (18), (26), (21)-(23) and (27) were used to simulate the batch case. As in the continuous case, the mass transfer between the polymer and the gas was described through the equilibrium concentration. Therefore, equation (20) was not included in the simulation. The convective terms in the mass and energy balance in the gas phase was discretized through the backward-finite differences. Due to the fact that the polymer phase is stationary, the convective term is absent in the mass and energy balance and no discretization was needed. The boundary conditions are applied as in the previous example. The inlet

boundary condition is specified while the boundary at the outlet was calculated through the model. There was no need for boundary conditions for the polymer phase, since nothing was discretized in these equations.

7.4 Single pellet model

Equation (20) including boundary conditions was used for the simulation of the diffusion in a single particle. This was performed as a separate simulation from the two above mentioned, using an example from the literature. In contrast to the previous simulations, the concentration in the polymer is assumed to vary with respect to the radius. The equation was discretized by the central finite-difference. All boundary conditions described for equation (20) were included in the simulation, and the model predicted the concentration profile. The reason for this is that the driving force for the diffusion, which is the concentration gradient between the polymer and the bulk phase, needed to be stated in the simulation. This is the concentration difference between the polymer and the surrounding media, the gas. In other words, the equilibrium concentration in the film at the polymer side is the boundary condition at rad.

8 Experimental data and parameter estimation

Looking at equation (18), (19) and (26) the mass transfer coefficient (k) needs to be estimated based on experimental data. The mass transfer coefficient describes the diffusion coefficient, the phase resistance between the pellet and the air and the effect of the air flow rate on the mass transfer. In the ideal case, separate sets of data would be used for the parameter estimation and validation but due to the lack of experimental data, the same data was used for both purposes. The heat transfer coefficients, seen in equations (23), (24) and (27), would also be estimated but due to the lack of experimental data of the energy balance, a value from the literature was used.

8.1 Experimental data

The validation data was received from pilot scale experiments ran on 1-5 types of grades of polymers produced by Borealis. Batch and continuous test runs were performed using hot air as stripping gas.

The same equipment was used for the batch and continuous runs. Figure 5 is a good representation of the equipment. In the continuous test the polymer phase was flowing through the equipment gravimetrically with a constant flow rate, while the gas phase was flowing from the bottom to the top, also with a constant flow rate. In the batch experiments, the outflow for the polymers was closed and the purge bin was filled with polymers, which means that the polymer phase stays stationary, while the gas was flowing through the polymers from the bottom to the top. The procedure for taking samples looks as follows for the continuous process. When the equipment was in steady state, the flows (gas and polymers) were stopped and samples were taken from the column in positions which corresponded to specific residence times. In the batch experiments, the samples were taken from the top of the column at specific times.

The FOG and VOC values, explained in section 2.3, were analysed, using the VDA278 test method, and therefore used in the estimation and simulation. Some features of the polymer grades are presented in a dimensionless form in Table 2 where all values are proportional to grade number 1.

Table 2. Properties of the polymer grades.

Grade	Density	Crystallinity	Bed porosity
1	1	1	1
2	1.05	1.03	1.01
3	1.08	0.97	1.2
4	1.07	1.06	1.01
5	1.07	0.9	1.3

Figure 10 and Figure 11 presents the dimensionless concentration of the experimental data of the continuous pilot experiments. The VOCs and FOGs are represented. As seen in section 2.3 FOGs represent hydrocarbons in the range of C14-C32 and the VOCs C1-C25. The concentration is dimensionless with respect to the initial concentration of each test and the time is dimensionless with respect to the total time. Possible outliers in the experimental data are shown with a red circle and the previous point, corresponding to the outlier, is shown with the arrow.

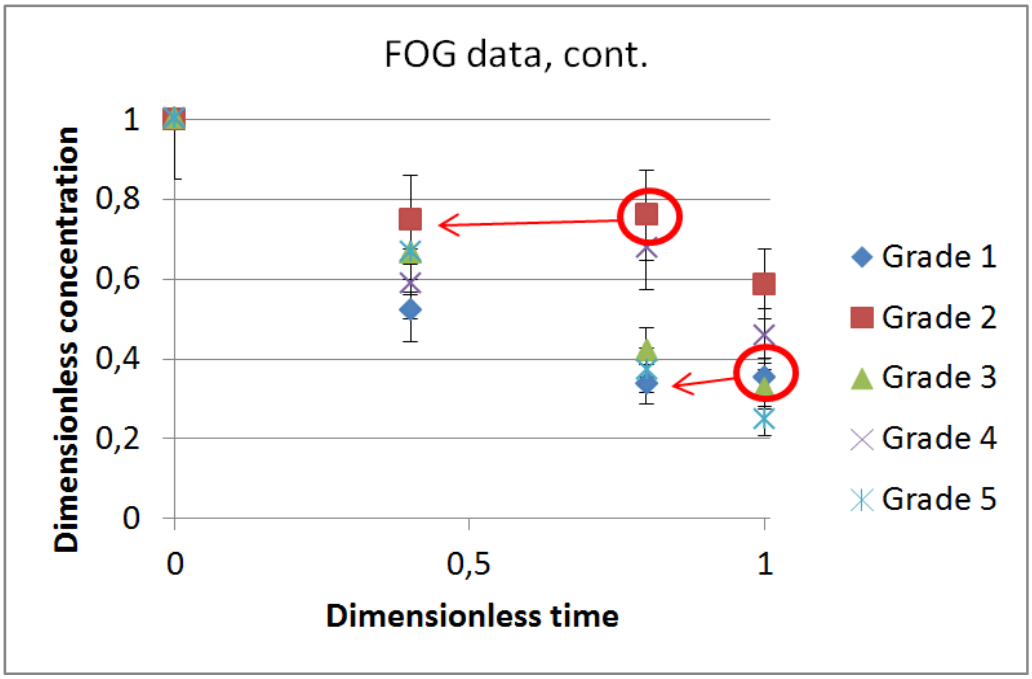

Figure 10. The experimental data of the continuous tests, FOGs.

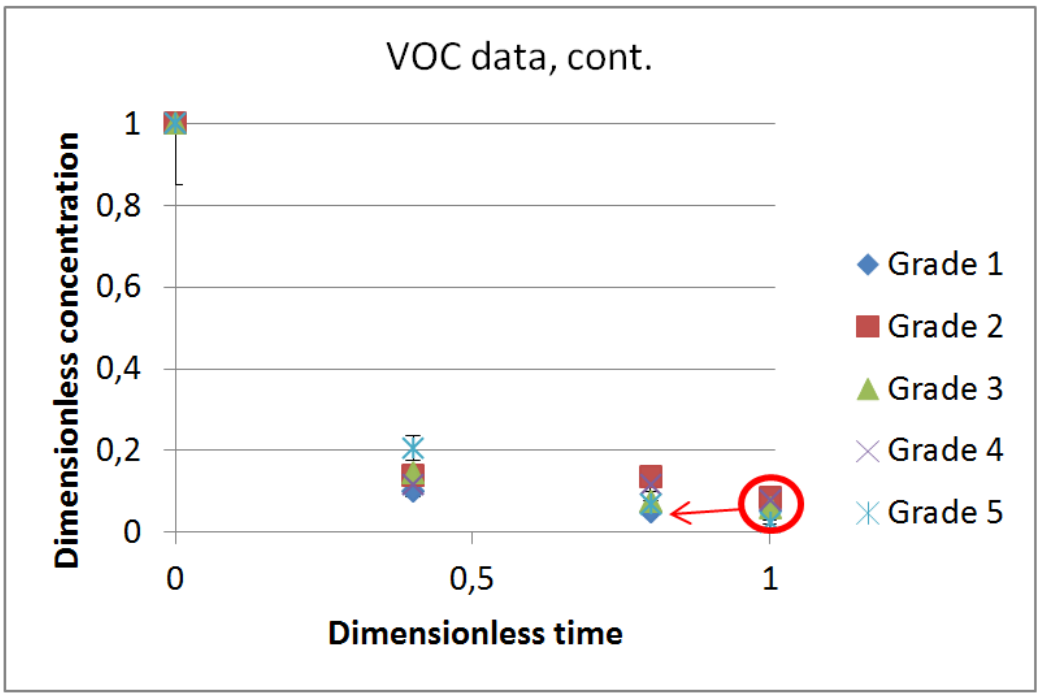

Figure 11. The experimental data of the continuous tests, VOCs.

Figure 12 and Figure 13 represents the dimensionless concentration of the experimental data of the batch experiments.

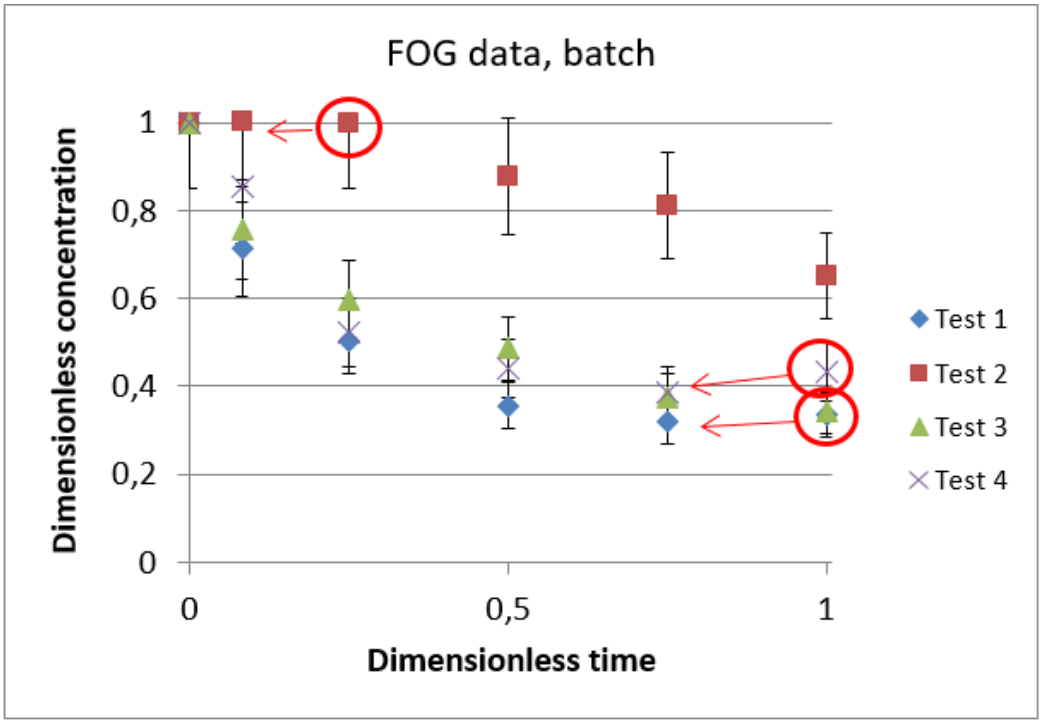

Figure 12. The experimental data of the batch tests, FOGs

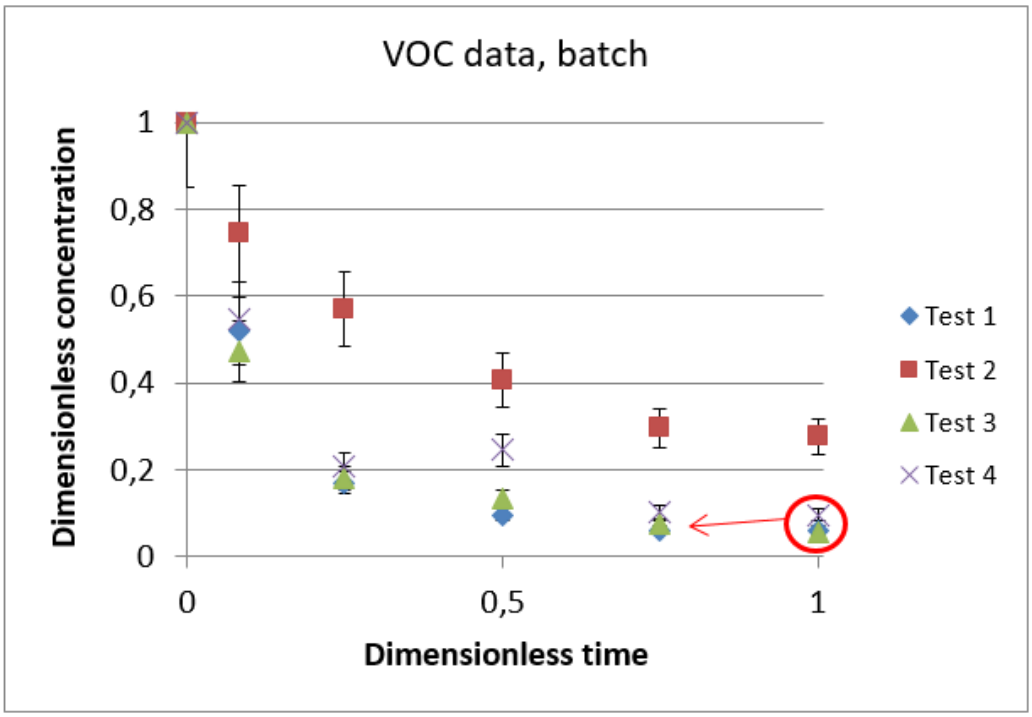

Figure 13. The experimental data of the batch tests, FOGs

In the case of the continuous data, five different grades were aerated in the same conditions (in terms of temperature, equipment dimensions, flow rates etc.). Looking at the continuous VOC data, all grades seem to follow a similar pattern and thus should the fitted mass transfer coefficient be good. Looking at the FOG data, the grades do not follow the similar pattern since grades 2&4 look different from grades 1,3&5. Unless the reason for the difference is found and added as a parameter to the model, one mass transfer coefficient cannot be expected to fit all grades well.

The same grade was used for all tests in the batch data, which was grade number 2. The air flow rate was changed between the runs, while the rest of the parameters were held constant. Four different tests were performed. The flow rates in the experiments were in the following order from the largest to the smallest 1&4, 3 and 2, 1 and 4 had the same flow rate. The diffusion curves differ from each other, both for the VOCs and FOGs, but the term for the velocity of the airflow should compensate for this.

8.2 Estimation of the mass transfer coefficient

The mass transfer coefficients were estimated separately for the FOGs and the VOCs. One mass transfer coefficient was estimated for the continuous case and one for the batch case,

using all of the available experimental data. An estimation tool available in ACM was used for the parameter fitting. The tool allows the different tests to have different condition in terms of fixed parameters.

8.2.1 Continuous

In the continuous case, the crystallinity and the density of the grades varied in the validation data, which was stated in the estimation tool. The estimation was done with four different approaches. First the model was tested with and without possible outliers in the experimental data. Secondly the term for the crystallinity was removed from the mass transfer equations (equations (18), (19) and (26)). Table 3 shows the obtained mass transfer coefficients with the corresponding confidence interval and the sum of weighted squared errors (SWSE) of the estimation. The mass transfer coefficients and SWSE are in dimensionless forms with respect to the estimation number 2. The confidence intervals are in dimensionless forms with respect to the mass transfer coefficient of each individual estimation. The weighted least squares method, seen in equation (28), was used for the parameter estimation. The SWSE is the sum of the error ($w_{ij}^2(z_{ij} - \hat{z}_{ij})^2 \; and \; w_{ijk}^2(z_j(t_{ijk}) - \hat{z}_{ijk})^2$) of equation (28).

$$\min_{\theta} \left\{ \sum_{i=1}^{N_{dyn}} \sum_{j=1}^{N_{meas}} \sum_{k=1}^{M_{ij}} w_{ijk}^2 (z_j(t_{ijk}) - \hat{z}_{ijk})^2 + \sum_{i=1}^{N_{ss}} \sum_{j=1}^{N_{Meas}} w_{ij}^2 (z_{ij} - \hat{z}_{ij})^2 \right\} \quad (28)$$

where θ corresponds to the estimated parameter, dyn to dynamic simulations, SS to steady-state simulations and Meas to measured values. The subscript i stands for simulated values, j for measured values and k for time. $\hat{z}$ is the calculated value and z the measured. w_{ij} are weights, which were all equal in the estimations of this work.

Table 3. The obtained mass transfer coefficients with confidence intervals and SWSE for the continuous case of FOGs and VOCs.

Estimation Case	Explanation	k, FOG	k, VOC	SWSE, FOG	SWSE, VOC
1	Outliers of the validation data included in the estimation, crystallinity excluded from model	0.21±1.26	0.21±1.32	0.91	1
2	Outliers of the validation data included in the estimation, crystallinity included in the model	1±1.27	1±1.32	1	1
3	Outliers of the validation data excluded from the estimation, crystallinity excluded from the model	0.23±1.29	0.22±1.37	0.74	0.9
4	Outliers of the validation data excluded from the estimation, crystallinity included in the model	1.04±1.32	1.06±1.37	0.89	0.9

As seen, the mass transfer coefficients of estimation number 1 and 3 are significantly smaller than that for 2 and 4. This is obvious since the term (1-y), which takes a number 0-1, in the mass balances is excluded in this case. The difference between estimation number 2 & 4 and 1 & 3 is small, which proves that the outliers have small effect on the estimation of the mass transfer coefficients. Looking at the SWSE of the FOGs, estimation number 3 has the best fit, 4 the second best, 1 third and 2 the worst. The pattern looks as follows: the removal of the outliers and exclusion of the crystallinity improve the fit. It was expected that the removal of possible outliers in the experimental data improves the fit. The fact that the fit is worse when the term for the crystallinity is present indicates that the mass transfer limitations are not only due to the crystallinity of the polymer. It is however important to state that the differences, in terms of mass transfer coefficient and SWSE, between the estimations are relatively small. The improvement in the SWSE does not show an improvement in the confidence interval. This means that even if the SWSE is smaller, the uncertainty of the optimal value of k is larger. The estimation of the VOCs follows the same pattern as the FOGs except that the elimination of the term describing the crystallinity does not improve the fit nor makes is worse. In other words, the crystallinity does not affect the de-volatilization of the VOC, according to these specific tests.

8.2.2 Batch

The velocities of the airflow varied between the experiments in the batch case, while the rest of the conditions remained the same. As in the continuous case, the differences between the tests were stated in the estimation tool. The estimation was done with two different approaches for the batch case. Since only one grade was used for all the tests of the batch case, there was no need for testing the model with and without the crystallinity. However, the cases with and without outliers of the validation data were tested. Table 4 shows the dimensionless mass transfer coefficients and confidence intervals for the FOGs and VOCs. The mass transfer coefficients and SWSE are in a dimensionless form with respect to test number 1. The confidence intervals are dimensionless with respect to the mass transfer coefficient of each individual test.

Table 4. The obtained mass transfer coefficients for the batch case of FOGs and VOCs.

Estimation number	Explanation	k, FOG	k, VOC	SWSE, FOG	SWSE, VOC
1	Outliers of the validation data included in the estimation, crystallinity included in the model	1±1.29	1±1.29	1	1
2	Outliers of the validation data excluded from the estimation, crystallinity included in the model	1.03±1.34	1.05±1.31	0.97	0.92

As in the continuous case, the difference between number 1 and 2 is small and thus do the outliers not affect the results of the parameter estimation significantly. Looking at the SWSE, the fit is marginally improved when the possible outliers are excluded for both the FOGs and VOCs. Also is these simulations, the confidence intervals are larger in the case with smaller SWSEs.

9 Simulation results

The same data, as described in section 8, was used for the validation of the performance of the model. The parameters estimated in section 8 were used for the mass transfer coefficient. Through this, the performance of the continuous and batch models, were investigated for each individual grade/run, using the same “global” continuous or batch mass transfer coefficient, found based on all continuous or all batch experiments. The mass transfer coefficients estimated with and without the outliers included were tested and also the case where the crystallinity was excluded from the model was simulated. The effect of the crystallinity term included and excluded in the mass balance will be presented in the continuous case, while the effect of the outliers in the experimental data will be presented in the batch case. The error bars in all plots are 15%, since this is the standard error of the procedures explained in section 2.3.

9.1 Continuous process and the effect of the crystallinity

In this section the results of the mass balance and the effect of the crystallinity on it is presented in the first section. The second section presents the results of the energy balance, only where the crystallinity is included. The simulations performed in this section are based on the experimental data without possible outliers.

9.1.1 Mass balance

The results of the continuous simulation are seen in Figure 14 – Figure 18. The left figure in each plot, represent the simulation of the model where the crystallinity term is absent and the right figure in each plot represents the simulation of the model where the crystallinity term is added in the mass transfer equations (18) and (19).

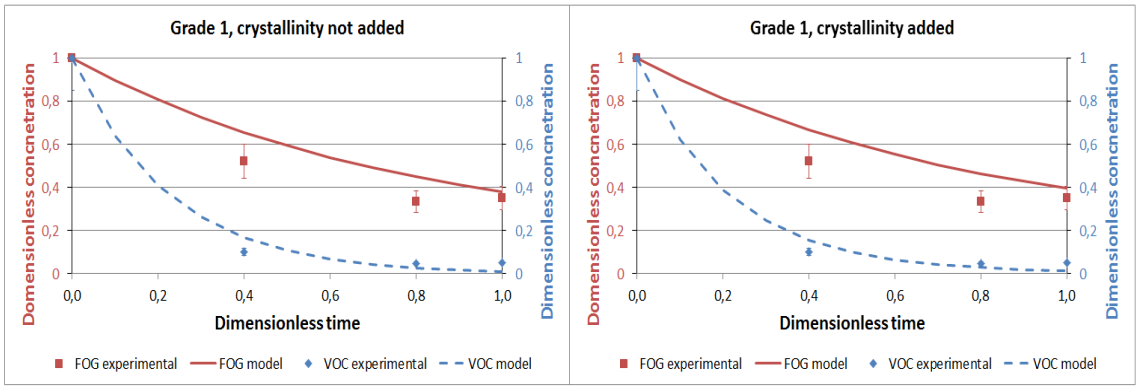

Figure 14. Simulation result of mass transfer of grade number 1, continuous.

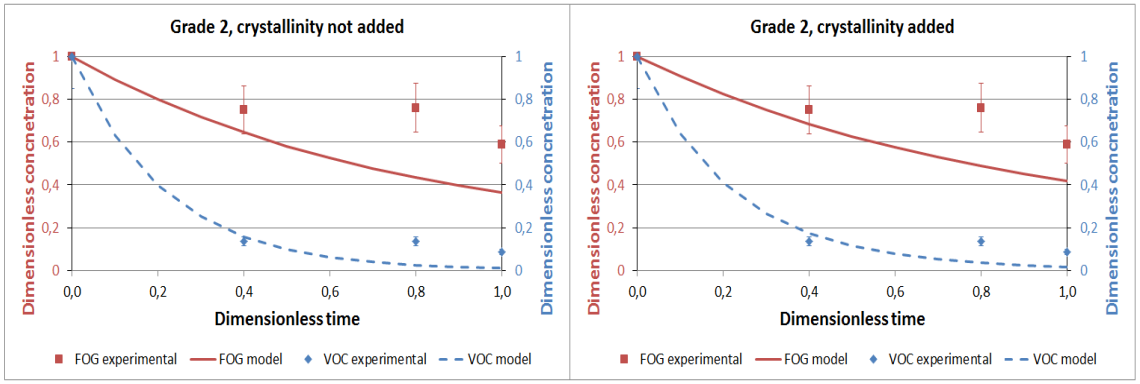

Figure 15. Simulation result of mass transfer of grade number 2, continuous.

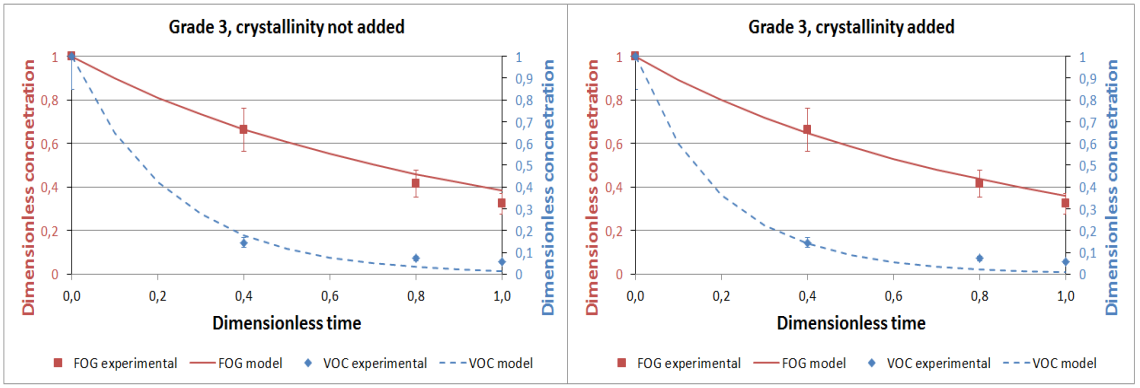

Figure 16. Simulation result of mass transfer of grade number 3, continuous.

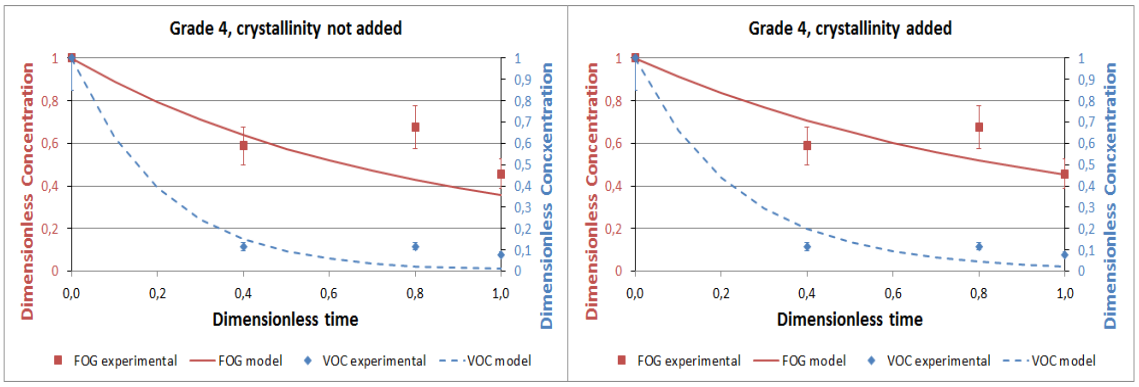

Figure 17. Simulation result of mass transfer of grade number 4, continuous.

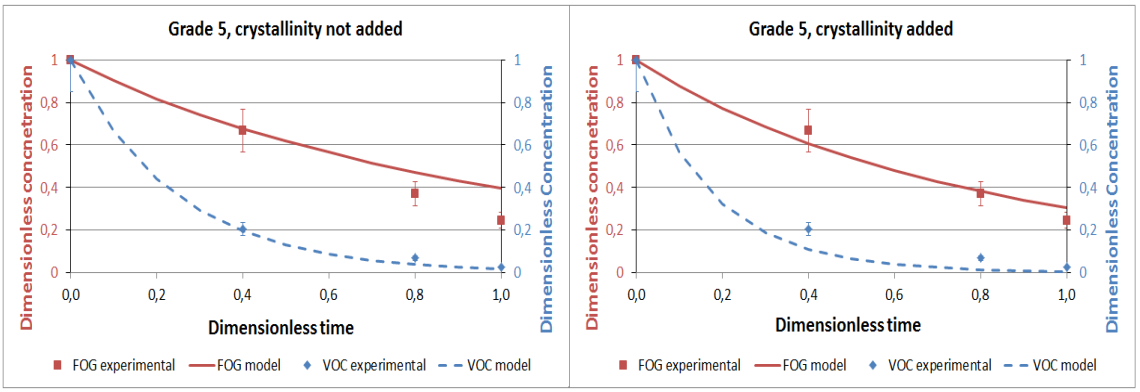

Figure 18. Simulation result of mass transfer of grade number 5, continuous.

In this specific case the comparison of results focuses on the FOGs rather than the VOCs. There are two reasons for this. The quantity of the VOCs is significantly smaller compared to the FOGs. Therefore, even small changes in the concentration of the VOCs create a large error, which is not realistic. The second reason concerns the degassing rate of the VOCs. It is clear that this is much faster compared to the FOGs and since the de-volatilization will be ongoing until also the FOGs are removed, the VOCs will for sure be removed at this time.

Comparing the different grades of the scenario without the crystallinity added, grades 3 and 5 have the best fit. Grades 2 and 4 have an acceptable fit in the first two points, but the curve should be less steep towards the end of the de-volatilization. This indicates that the rate of mass transfer is of larger quantity in the beginning of the de-volatilization, and decreases towards the end. Grade 1 has an acceptable fit in the first and last point but, also in this case, the curve should be less steep towards the end of the de-volatilization, as for grade 2 and 4. Looking at the properties of the polymers in Table 2, grade 3 and 5 have the lowest crystallinity. This might explain the better fit for these specific grades, compared to the rest

of the grades. Another fact worth mentioning is that grades 1, 2 and 4 are the ones containing possible outliers in the experimental data. This is of big significance since the mass transfer coefficient is estimated entirely based on the experimental data.

Looking at the scenarios with the crystallinity added, the same grades as for without the crystallinity added have the best fits. According to the SWSE found in Table 4, the fit should be slightly worse in the figures on the right compared to the figures on the left. This is however not seen with only eyes, except for grade number 1. It is questionable if the fit is worse for all grades when the crystallinity is added, or if the fit of grade number 1 is significantly worse and therefore raises the SWSE of the estimation. Further, the same issue is present in all cases, as mentioned above, about the de-gassing curve being too steep in the end and too flat in the beginning of the de-volatilization.

The mass balance for the FOGs was tested by estimating separate mass transfer coefficients for each grade. The outliers in the experimental data were kept and the crystallinity was included in the model. Better results are obtained as can be seen in the figures in appendix 1.

9.1.2 Energy balance

The results of the energy balances are seen in Figure 19 - Figure 21. These represent the dimensionless temperature of the gas and polymer phases as a function of the dimensionless time. The temperature is dimensionless with respect to the initial temperature in ^{o}C of the gas and the time is dimensionless with respect to the total residence time. The crystallinity does not affect the energy balance, which is seen in equations (23), (24) and (27). Therefore, only one set of results are presented here. No validation data was available on the energy balance and therefore only plots on the simulated results are presented. The heat transfer coefficient seen in equations (23), (24) and (27) was chosen as a value from the literature (31) (32).

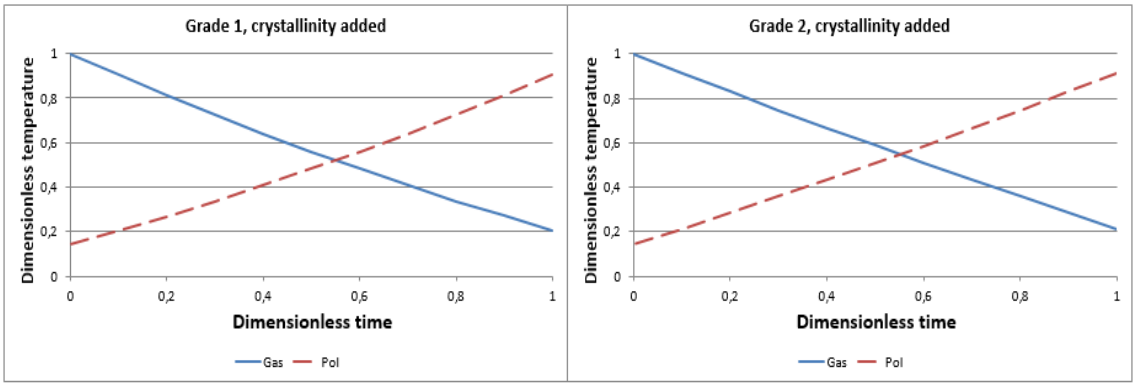

Figure 19. Simulation results of energy balance, grade 1 and 2.

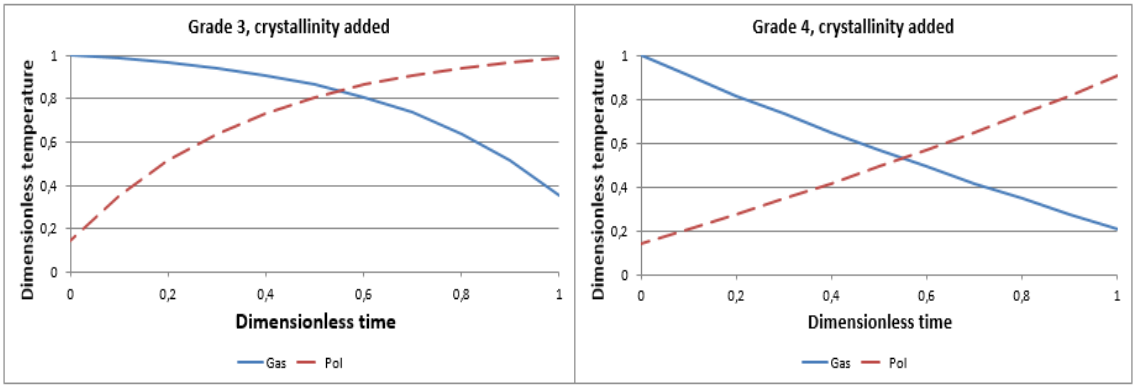

Figure 20. Simulation results of energy balance, grade 3 and 4.

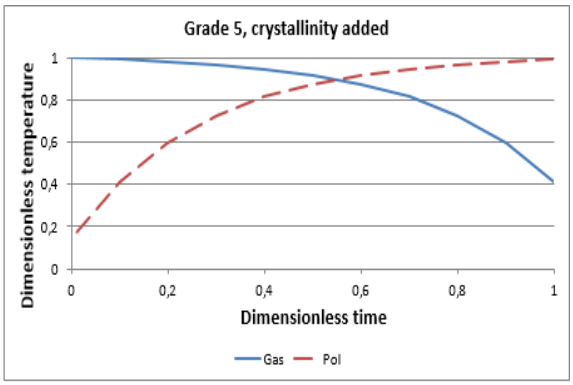

Figure 21. Simulation results of energy balance, grade 5.

Comparing the figures, grade number 1, 2 and 4 give results close to each other while grade number 3 and 5 give similar results. It is visible in the plots of grade 1, 2 and 4 that the temperature of the gas decrease fast and the temperature of the polymer increase slowly compared to the plots of grade 3 and 5. Looking at Table 2, grade number 3 and 5 have a high bed porosity compared to the rest of the grades. The high bed porosity means that the

gas to polymer ratio is larger in each control volume and the velocities of the flows of the medias are affected. The density of the polymer affects the energy transfer in the sense that the bed porosity partially depends on the density of the polymer. The shape and size of the polymer pellet has, however, a bigger impact on the porosity of the bed.

9.2 Batch process and the effect of outliers

In this section the results of the mass balance and the effect of the outliers, in the validation data, is presented in the first section. The second section presents the results of the energy balance.

9.2.1 Mass balance

The results of the batch simulations are seen in Figure 22 - Figure 25. The left figure in each plot represents the scenario, in which possible outliers are eliminated from the experimental data. The outliers are excluded from both the data used in the parameter estimation and validation. The figure on the right side represents the simulation, based on the data where possible outliers are included in both the estimation and validation.

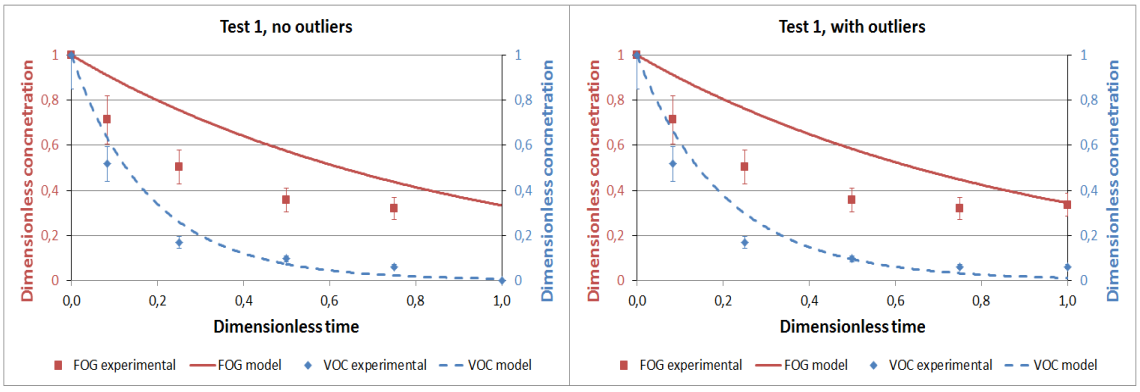

Figure 22. Simulation results of mass transfer of test number 1, batch.

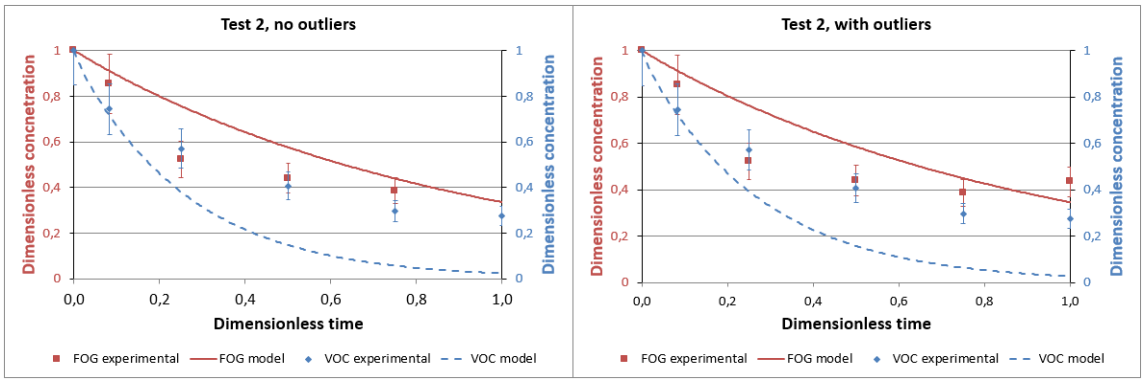

Figure 23. Simulation results of mass transfer of test number 2, batch.

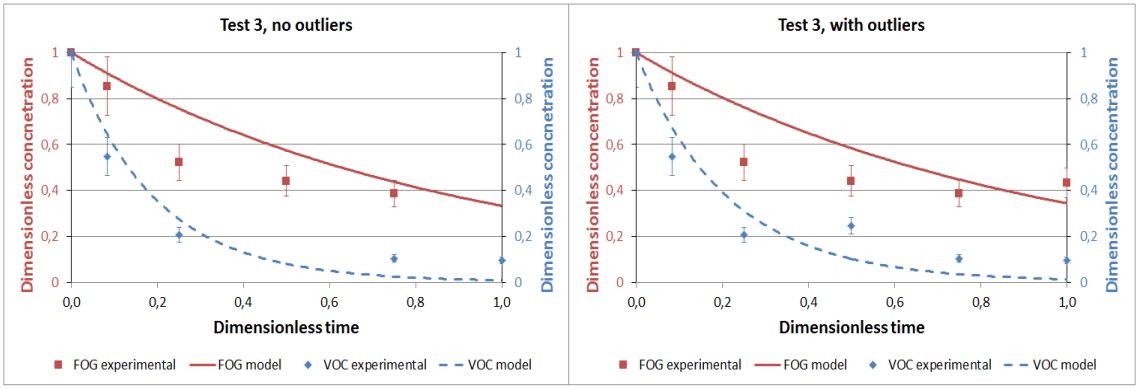

Figure 24. Simulation results of mass transfer of test number 3, batch.

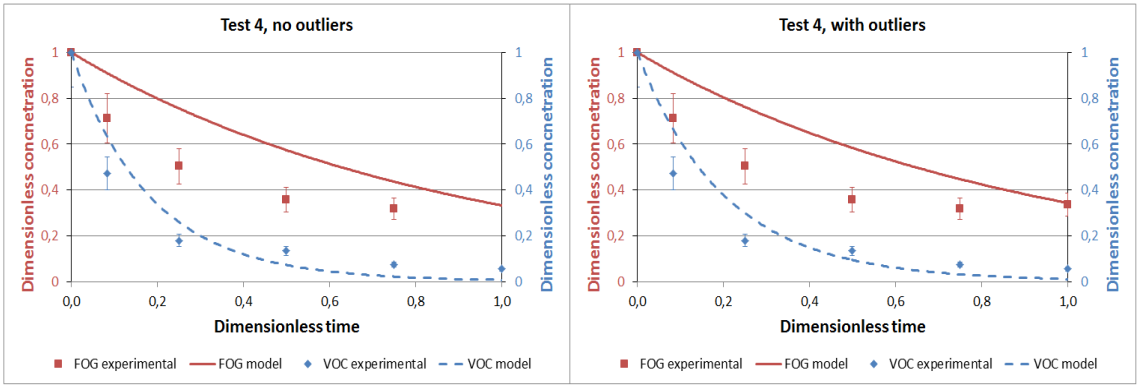

Figure 25. Simulation results of mass transfer of test number 4, batch.

As explained in the previous section, this specific case focuses on the de-volatilization of the FOGs rather than the VOCs.

Looking at the right figure of all plots, the same issue is present in every case. The de-volatilization curve of the simulated data is too flat in the beginning of the degassing and too steep in the end. This means that the mass transfer in the experimental data is faster in the

beginning of the de-volatilization, compared to the end of the test. The same issue was seen in the previous section but it is more significant here. As explained in section 8.1, test 1 and 4 has the highest flow rate, 3 have the second highest and 2 have the lowest. Test 1 and 4 seem to have a better fit towards the end of the de-gassing while test 2 and 4 has better fit in the beginning. This means that the high gas flow rate shows especially fast initial decrease of the hydrocarbons. The low gas flow rate show an especially slow decrease of the hydrocarbons in the end of the de-volatilization.

The difference between the right and left figure of all tests is small and cannot be seen with only eyes. This was expected since the difference between the mass transfer coefficients, of the case where the possible outliers are excluded and included are similar, as seen in Table 4. The possible outlier in all graphs is the last point, which seems to be too large compared to the second last point. Since the de-gassing curve seems to be too steep in the end of the de-gassing, the fact that the last point is eliminated makes the fit look better. It cannot, however, be stated that the fit actually is better is this case, since the last point is unknown.

The mass balance for the FOGs were tested by estimating separate mass transfer coefficients for each grade. The outliers in the experimental data was kept and the crystallinity was included in the model. The results showed better results compared to the case described above, as expected. The results could, however, be improved by modelling the mass transfer coefficient in such way that the gas flow rate would be included. The results are seen in appendix 1.

9.2.2 Energy balance

The results of the energy balances are seen in Figure 26 and Figure 27. As in the continuous simulation of energy balances, no validation data was available for the batch case. This means that the energy balance was not simulated with and without outliers and the heat transfer coefficient was chosen from the literature. As explained in section 8.1, pre-heating took place in all tests 1-4 of the batch cases. Figure 26 represents the temperature profile of different axial position in the purge bin, 0 being the bottom where the gas enters the vessel and 1 being the top where the gas leaves the vessel, with the gas flow rate of the pre-heating phase of the polymer. Figure 27 represents the energy balance of a lower gas flow rate (24% of the higher air flow rate).

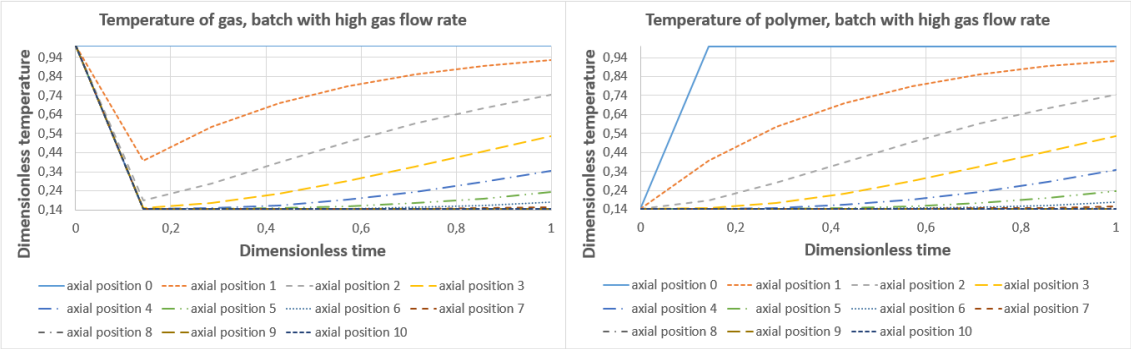

Figure 26. Simulation results of energy balance, higher gas flow rate.

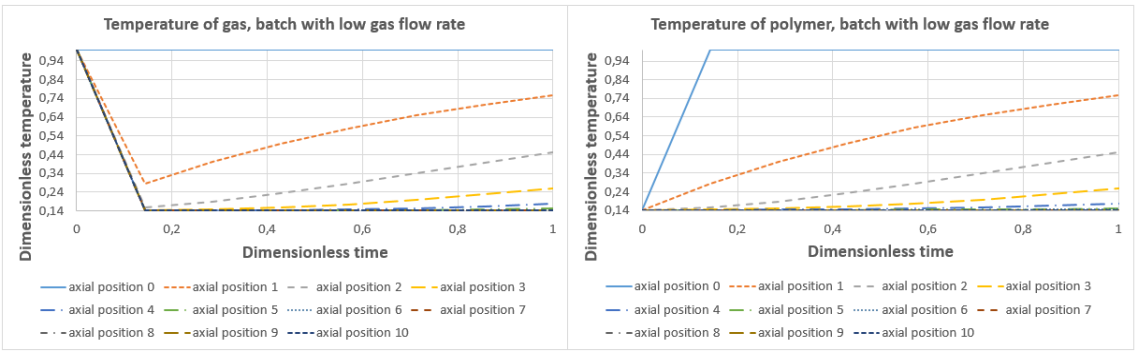

Figure 27. Simulation results of energy balance, lower gas flow rate.

Looking at Figure 26, each of the axial positions reaches the highest temperature of dimensionless value of 1 after a certain time, which is the temperature of the gas. In this figure, all control volumes do not reach the dimensionless temperature of 1 but it is only due to the short aeration time. If the aeration time would be continued, also these axial positions would reach the dimensionless temperature of 1. It is visible that the control volume closest to the gas inlet is heated to 1 first, which after the control volume second closest to the inlet is heated and so on. This is because the energy of the gas is used to heat up the specific control volume and is therefore significantly lower when reaching the next control volume. When the previous control volume is already heated, the temperature of the gas stays constant and may heat up the second control volume. This results in the pattern seen in the figures above. Comparing the higher and lower gas flow rate, the same phenomenon is visible but the heating is slower for the case with a lower gas flow rate. This is obvious since the convective term, of the energy balance of the gas phase, is decreasing when the gas flow rate is decreasing. Comparing the gas and polymer graphs, they look similar except that the gas has a higher temperature when entering the vessel, which is then dropped

before being heated up in each control volume. The polymer phase has a lower temperature when entering the vessel before being heated up to the temperature of the gas.

9.3 Single particle model

The single particle model was simulated as a possible scenario in the industry, based on data from the literature. This means that the particle size and the initial impurity concentration were chosen as values, which could generally be found for industrial polymers according to the literature, but no validation data is available on this. The simulation was performed as explained in section 7.4 and Table 5 shows the values used for the parameters. (31)

Table 5. Values for the simulation of the single particle.

Parameter	Value	Unit
Particle diameter	0.008	cm
Temperature	140	°C
Diffusion coefficient	$1 \cdot 10^{-5}$	m^2/s

The diffusion coefficient was found from the literature and represents hexane in polypropylene. (31)

Figure 28 shows the evolution of the concentration in specific radial positons of the polymer particle, as a function of time. The same case is represented as a 3D plot in Figure 29. Here the radial position is represented as control volumes with 0 being the centre of the pellet and 50 the outer surface of the pellet. A difference is, however, that Figure 28 shows the simulation for 7 hours while Figure 29 shows the simulation for 2,5 hours, since the results are represented better in a 2,5 hour simulation.

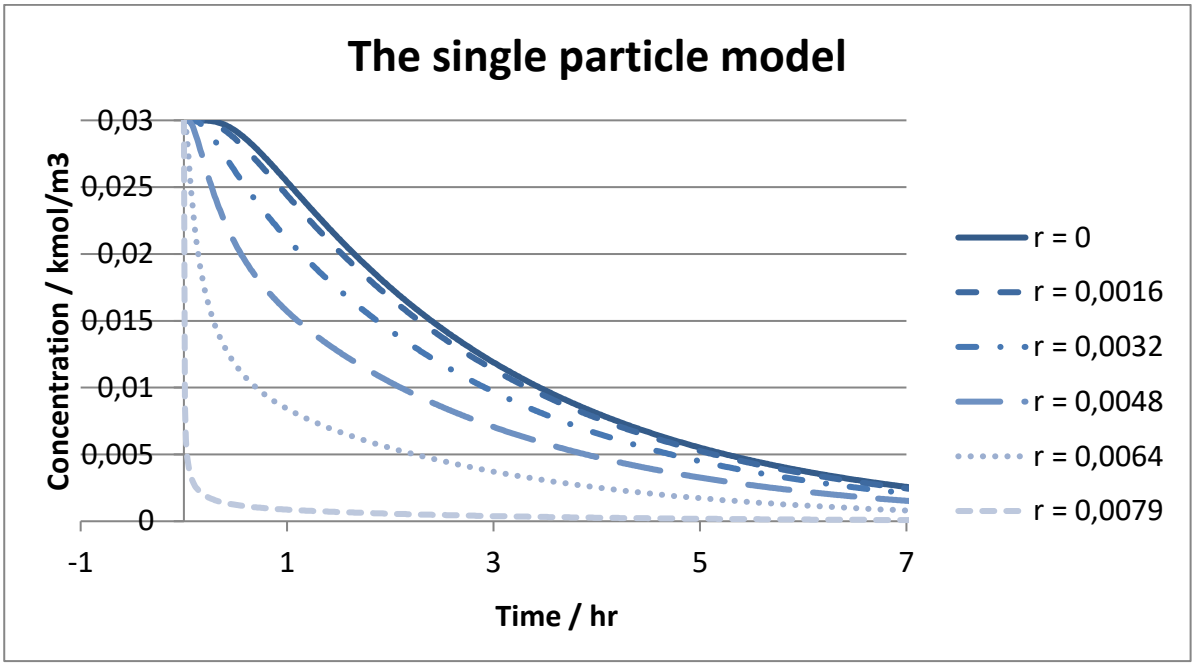

Figure 28. The evolution of the concentration in a single pellet.

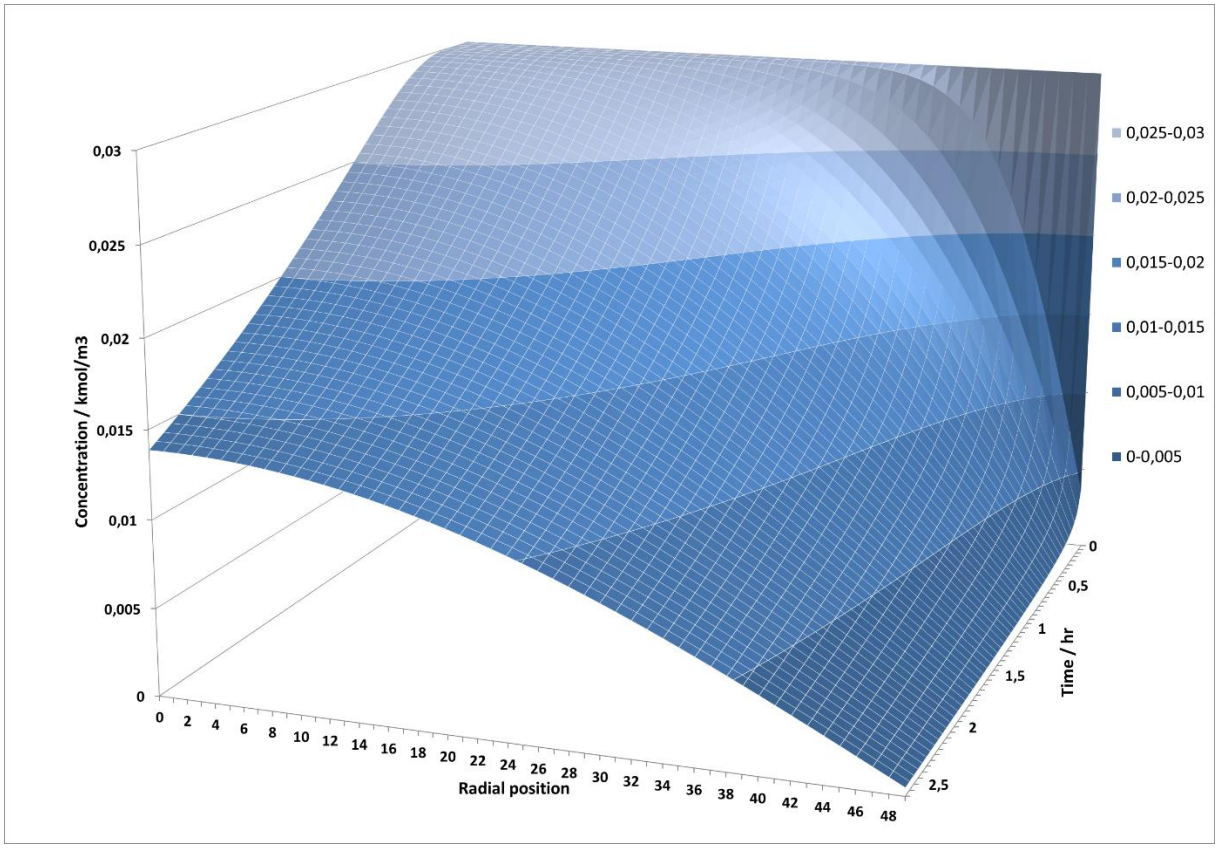

Figure 29. The evolution of the concentration in a single pellet as a function of time and radial position.

As expected, the hydrocarbons closer to the surface of the pellet, leave the pellet faster than the ones closer to the centre. Looking at Figure 28, the reduction of the hydrocarbons is fast in the beginning. This indicates that the diffusion is time dependent, in the sense that the hydrocarbons closest to the surface of the pellet leave the pellet faster. This should be taken into consideration in the mass transfer coefficient in equations (18), (19) and (26).

10 Conclusions

Polymers often contain impurities in the form of volatile organic compounds. These should be removed from the final product due to the market sensitivity and environmental regulations towards these substances. The substances can be removed in purge bins. In this thesis the Industrial purge bins were studied in continuous and batch modes. These were modelled, numerically solved and simulated with Aspen Custom Modeller. Experimental data was available for parameter estimation. The goal of the thesis was to be able to simulate industrial purge bins targeting different objectives as optimizing the process and sizing the equipment.

The experimental data was used to estimate the mass transfer coefficient for the mass balance and for comparison of the model prediction and the experimental data. The mass balance satisfied the experimental data of both the continuous and batch models. The following problem was however seen in both cases. The experimental data has a fast decrease of the hydrocarbons in the polymer phase in the beginning of the purging and a slower decrease (in relation to the beginning) towards the end, which is depicted by the simulations for both scenarios but to less extent than it should. Two different approaches in the mass balance and parameter estimation were taken. The experimental data including and excluding possible outliers were tested and the model including and excluding the term describing the crystallinity were tested. It was found that the presence of the term describing the crystallinity did not improve the results. There are two possible reasons for this. There might be other factors affecting the diffusion more than the crystallinity. Another reason might be that the fit was worse for a specific grade, increasing the SWSE, when adding the crystallinity, while the fit of other grades were improved.

The energy balances were simulated but due to the lack of experimental data, no coefficients were estimated and the model could not be compared to experimental data. A heat transfer coefficient found in the literature was used. The results of the energy balance looked as expected. The results show that bed porosity and the flow rate of the gas effected (and polymer phase in the case of the continuous process) the energy balance in the silo. Experimental data is needed to verify the findings in this work.

The single particle model based on Fick’s law was simulated. No validation data was available for this. The model shows the evolution of the concentration of the hydrocarbons

as a function of the radius of each individual polymer particle. The results showed that the hydrocarbons closer to the surface of the pellet diffuse, and therefore leave the pellet, significantly faster than the hydrocarbons closer to the centre of the pellet.

11 Suggestions for further research

The biggest issue in this study was the small amount of experimental data. Similar experiments as described in the validation data sections were ongoing during the duration of this thesis but were not received in time to include in the parameter estimation and comparison of the results. It is, however advisable to use the data in order to have different data for parameter estimation and model validation. Further, if validation data would be available for the energy balance, the heat transfer coefficient could be estimated based on this.

The effect of the temperature of the gas and polymer is visible in the energy balance but the mass balance is not affected much of this. This could be fixed by making the mass transfer coefficient temperature dependent in an Arrhenius type equation. This would require experimental data from different temperatures.

It was seen in the experimental data of the batch case that the flow rate of the gas has a big impact on the de-volatilization. The model took the flow rates of the media in to account through the convective term but as it was seen in the results, this was not enough to emphasis the flow rate dependency of the mass transfer. The mass transfer coefficient should be modelled as gas flow rate dependent.

As mentioned in the conclusions, the mass transfer of the impurities is larger in the beginning of the purging compared to the end, which was also seen in the single pellet model. This means that the mass transfer coefficient could be modelled as time dependent, which would indicate that the mass transfer decreases with time.

Fick's law of diffusion works nicely as a representation of the diffusion of the hydrocarbons in the polymer. When modelling the equilibrium concentration of the polymer, Fick's law could be added to the mass balance. Not only because the diffusion would become time dependent through this, but also because there is more data available in the literature on the diffusion coefficient compared to the mass transfer coefficient.

Notation

Bo	Bondenstein number
c	concentration
C_p	specific heat
D	diffusion coefficient
G	mass flow per unit cross section
H	Henrys constant
h	The height of the equipment
h_p	gas-solid heat transfer coefficient
h_v	volumetric heat transfer coefficient
ΔH	vaporisation heat of hydrocarbons
k	mass transfer coefficient
P	pressure
q_p	desorption rate of hydrocarbons
R	ideal gas constant
r	radial position in the polymer pellet
rad	radius of the polymer pellet
s_v	surface to volume ratio of polymer
T	temperature
t	time
v	velocity
x	position in the equipment

X	weight fraction of VOCs
$\overline{X}$	average weight fraction of VOCs
y	Crystallinity

Subscripts

eq	equilibrium
g	gas
i	hydrocarbon
p	polymer
s	solid
sp	single particle

Greek letters

ε	porosity of the bed
ρ	density
η	phase ratio
γ	phase resistance number

12 References

1. **Meier, Dirk, Warnecke, Hans-Joachim and Prüss, Jan.** Modelling of mass transfer of volatile organic compounds. *Chemical Engineering Journal.* 2 1 1997, pp. 45-53.

2. **United States Environmental Protection Agency.** ***Technical Overview of Volatile Oragnic Compounds.*** **[Online] United States Environmental Protection, 12 4 2017. [Cited: 2 8 2017.] https://www.epa.gov/indoor-air-quality-iaq/technical-overview-volatile-organic-compounds.**

3. Chen, Z, et al. Modelling and simulation of extraction of oligomer from granular polymers. ***Chemical Engineering Journal.*** **14 7 1997, pp. 165-172.**

4. Barandiaran, Maria J and Asua, Jose M. Removal of Monomers and VOCs from Polymers. ***Handbook of Polymer Reaction Engineering .*** **2008, pp. 971-994.**

5. Araûjo, P.H.H, et al. Techniques for Reducing Residual Monomer Content in Polymers: A Review. ***Polymer Engineering and Science.*** **7 2002, pp. 1442-1268.**

6. What does VOC mean? [Online] Scientific, Eurofins, 25 10 2016. [Cited: 7 6 2017.] http://www.eurofins.com/voc.aspx.

7. Volatile Organic Compounds' Impact on Indoor Air Quality. [Online] Agency, United States Environmental Protection, 19 4 2017. [Cited: 7 6 2017.] https://www.epa.gov/indoor-air-quality-iaq/volatile-organic-compounds-impact-indoor-air-quality.

8. Cinstable, John, Guenther, Alex and Schimel, David. Modelling changes in VOC emission in response to climate change in the continental United States. 10 1999, Vol. 5, 7, pp. 791-806.

9. Che, Jinshui, et al. ***Determination of Volatile COmpounds in Automotive Interior Materials by Thermal Desorption.*** **s.l. : Thermo Scientific, 2014.**

10. Shimadzu Europa GmbH. [Online] [Cited: 13 10 2017.] https://www.shimadzu.eu/sites/default/files/sca_280_081_analysis_of_voc_and_fog_according_to_vda278.pdf.

11. Shimadzu VDA 277: Analysis of Volatile Contaminants from Polymers. ***Shimadzu Application news.*** **[Online] [Cited: 23 10 2017.] https://www.shimadzu.eu/sites/default/files/vda_277-analysis_of_volatile_contaminants_from_polymers_sca_180_019.pdf.**

12. Soney, George C. and Sabu, Thomas. Transport phenomena through polymeric systems. ***Progress in Polymer Science.*** **28 7 2000, 26, pp. 985-1017.**

13. Danckwerts, P.V. Significance of Liquid-Film Coefficients in Gas Adsorption. 1951, pp. 1461-1467.

14. Zubov, Alexandr, et al. Transport and reaction in reconstructed porous polypropylene particles: Model validation. 2010, 65, pp. 2361-2372.

15. Seda, Libor, et al. Transport and Reaction Characteristics of Reconstructed Polyolefin Particles. 2008, Vol. 2, pp. 495-512.

16. Vreantas, J.S. and Duda, J.L. Diffusion of Small Molecules in Amorphous Polymers. 1976, Vol. 9, 5.

17. *Critical Phenomena in Gases. I.* Lennard-Jones, J. E. and Devonshire, A. F. 912, s.l. : Royal Society, 11 1937, Proceedings of the Royal Society of London. Series A, Mathematical and Physical Sciences, Vol. 163, pp. 53-70.

18. Kanellopoulos, Vassileios, et al. An Experimental and Theoretical Investigation into the Diffusion of Olefins in Semi-Crystalline Polymers: The Influence of swelling in Polymer-Penetrant Systems. 2007, Vol. 1, pp. 106-118.

19. Bobak, Marek, et al. Estimation of Morphology Characteristics of Porous Poly(propylene) Particles from Degassing Measurements. 2008, 2, p. 176189.

20. Whitaker, Stephen. Flow in Porous Media I: A Theoretical Derivation of Darcy's Law. 1986, 1, pp. 3-25.

21. Chen, Zhong, et al. Removal of Organic Impurities from Polymer Pellets. *Chemical Engineering Technology.* 2001, Vol. 24, pp. 523-528.

22. Sander, R. Compilation of Henry's law constants (version 4.0) for water as solvent. 2015, pp. 4399-4981.

23. Colakyan, M. and Eisinger, R. S. Removal of Residual Monomers from Polymers in Fluidized Beds. 2003, pp. 2654-2660.

24. Guarita, M. B., Secchi, A. R. and Marczak, L. D.F. *Stripping Hydrocarbons From Linear Low Density Polyethylene.* Costa Verde : ResearchGate, 2017.

25. Wang, Duan-Fan. *Process for removing unpolymerized gaseous monomers from olefin polymers. 5292863* United States, 8 3 1994.

26. Pittenger, B. H., et al. Uniform Purging of Resins in Contact Bed Purge Vessels. 9 1999, Vol. 39, 9, pp. 1802-1811.

27. Cozewith, Charles. Diffusion from Spherical Particles in a Continuous Flow Stirred Tank Train. 1994, 33, pp. 2712-2716.

28. Hänchen, Markus, Brückner, Sarah and Steinfeld, Aldo. High-temperature thermal storage using a packed bed of rocks e Heat transfer. 2011, pp. 1798-1806.

29. Hazewinkel, Michiel. Encyclopedia of Mathematics. *Parabolic partial differential equation, numerical methods.* [Online] 30 11 2014. [Cited: 1 8 2017.] https://www.encyclopediaofmath.org/index.php/Parabolic_partial_differential_equation,_numerical_methods.

30. Chapra, Steven C. and Raymond, Canale P. Numerical Differentation. *Numerical Methods for Engineers.* New York : McGraw-Hill, 2010, pp. 653-668.

31. Tan, So. SCRBD. *Heat Exchangers of Polypropylene.* [Online] 21 11 2012. https://www.scribd.com/document/113995541/Heat-Exchangers-of-Polypropylene.

32. Conti, Rosaria, Gallitto, Aurelio and Fiordilino, Emilio. *Measurement of the convective heat-transfer coefficient.* Palermo : Universita di Palermo, 2014.

33. Scicolone, James, et al. Solubility and diffusivity of solvents by packed column inverse gas chromatography. 2006, 47, pp. 5364-5370.

34. Kanellopoulos, V., et al. Evaluation of the Internal Particle Morphology in Catalytic Gas-Phase Olefin Polymerization Reactors. 22 2 2007, 46, pp. 1928-1937.

35. Quadri, G. P. Purification of Polymers from Solvents by Steam or Gas Stripping. 1998, 37, pp. 2850-2863.

36. Salazar, Rafael, et al. Post-polymerization vs devolatilization for monomer removal in latexes. 2004, 124, pp. 116-120.

37. Kechagia, Zoi, et al. A Kinetic Investigation of Removal of Residual Monomers From Polymer Latexes Via Post- polymerization and Nitrogen Stripping Methods. 2011, 5, pp. 479-489.

38. Chen, Meijuan, et al. Diffusion Measurements of Isopentane, 1-Hexene, Cyclohexane in Polyethylene Particles by the Intelligent Gravimetric Analyzer. 2013, pp. 1096-1104.

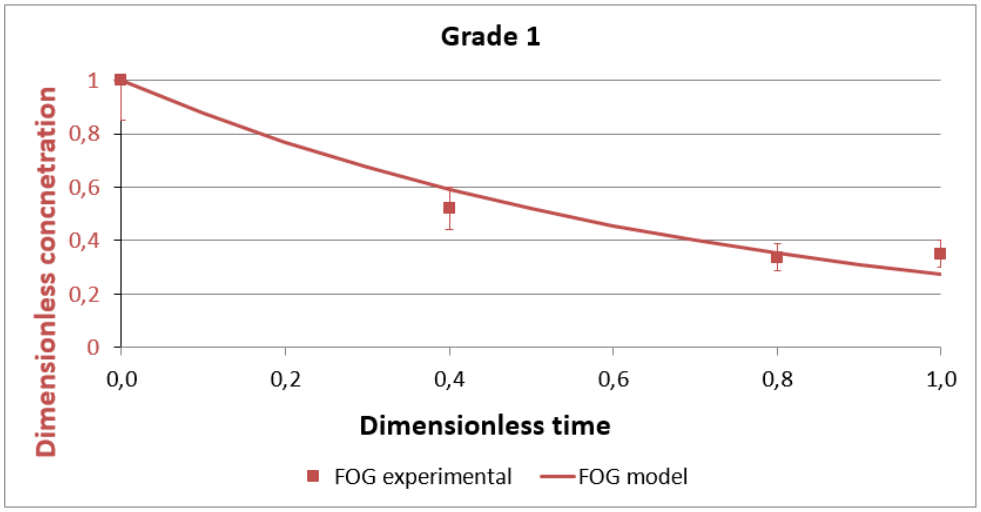

Figure 30. Simulation result of mass transfer of grade number 1, continuous and mass transfer coefficient estimated based on grade number 1.

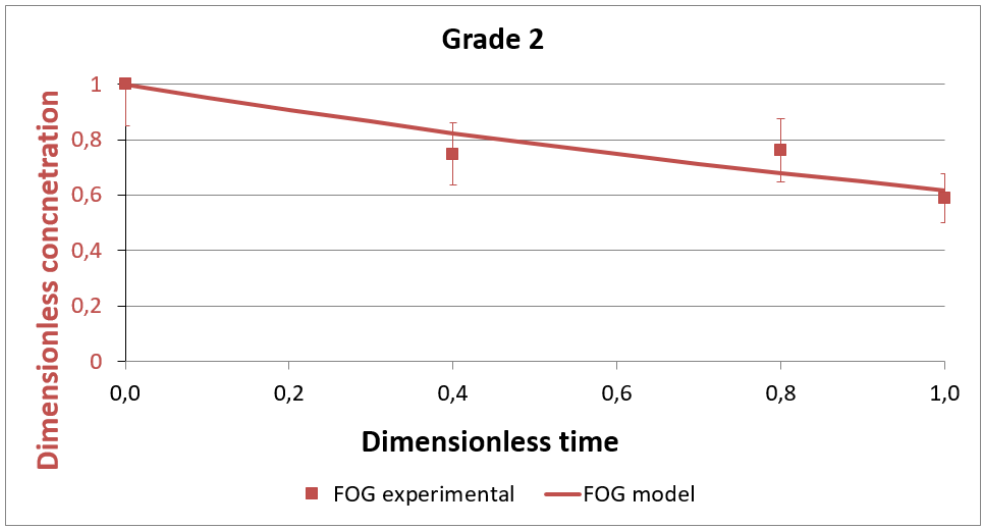

Figure 31. Simulation result of mass transfer of grade number 2, continuous and mass transfer coefficient estimated based on grade number 2.

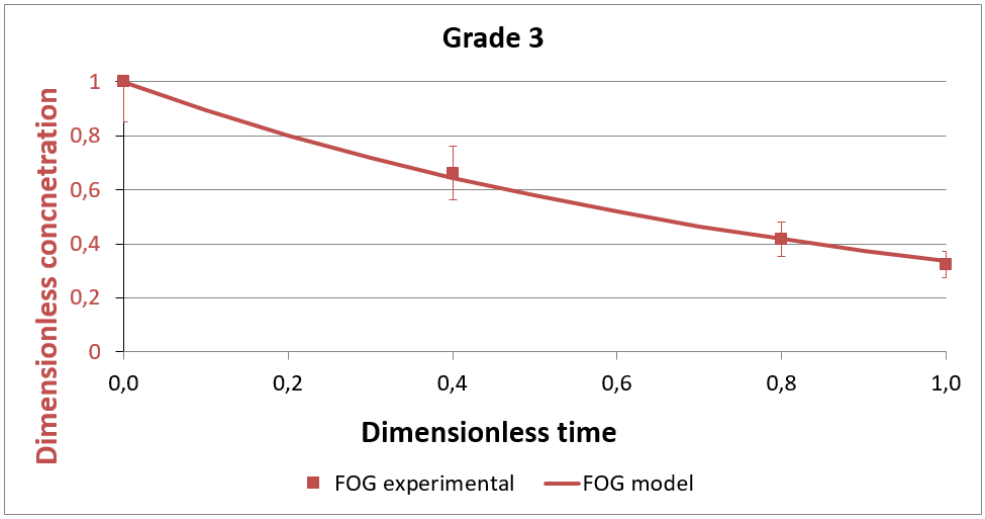

Figure 32. Simulation result of mass transfer of grade number 3, continuous and mass transfer coefficient estimated based on grade number 3.

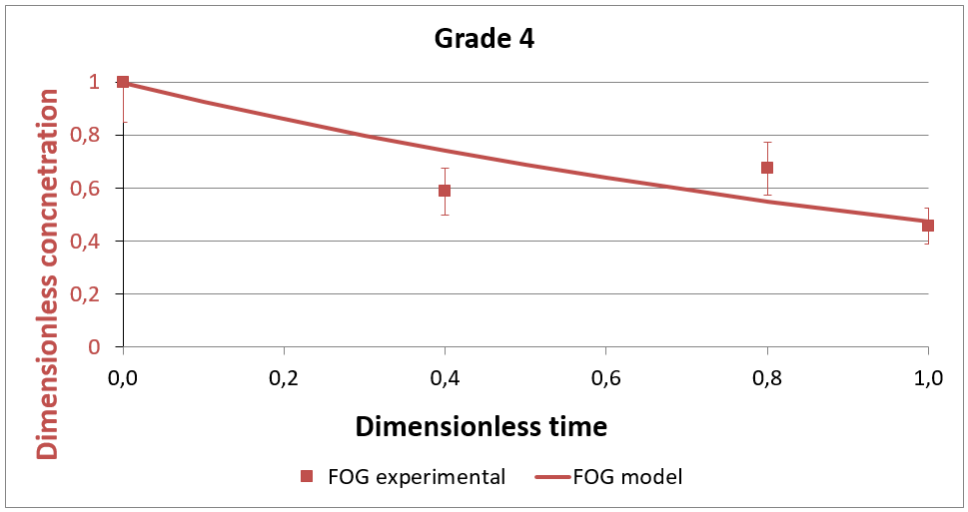

Figure 33. Simulation result of mass transfer of grade number 4, continuous and mass transfer coefficient estimated based on grade number 4.

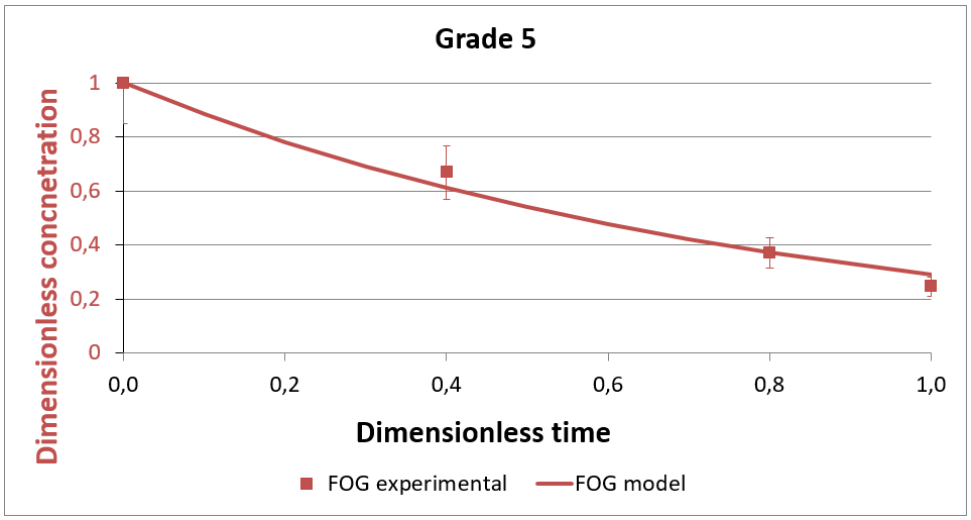

Figure 34. Simulation result of mass transfer of grade number 5, continuous and mass transfer coefficient estimated based on grade number 5.

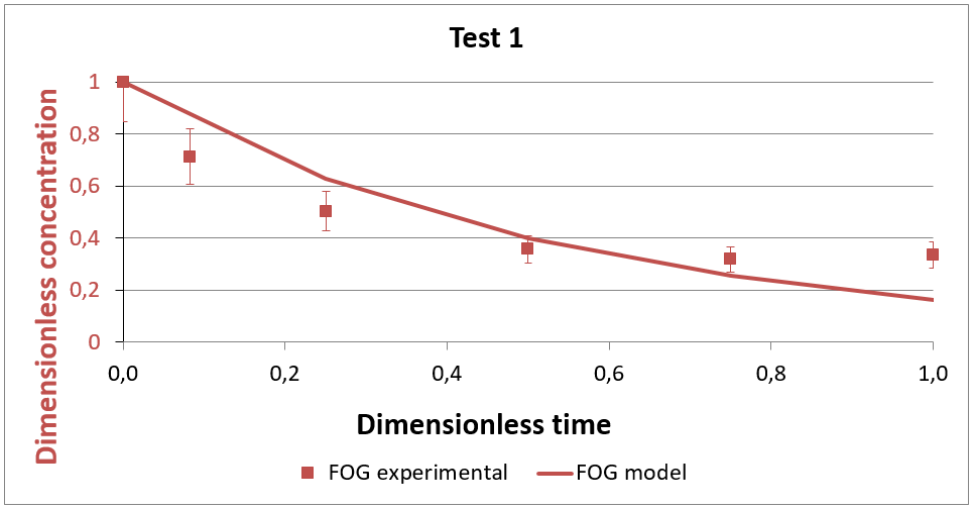

Figure 35. Simulation result of mass transfer of test number 1, continuous and mass transfer coefficient estimated based on test number 1.

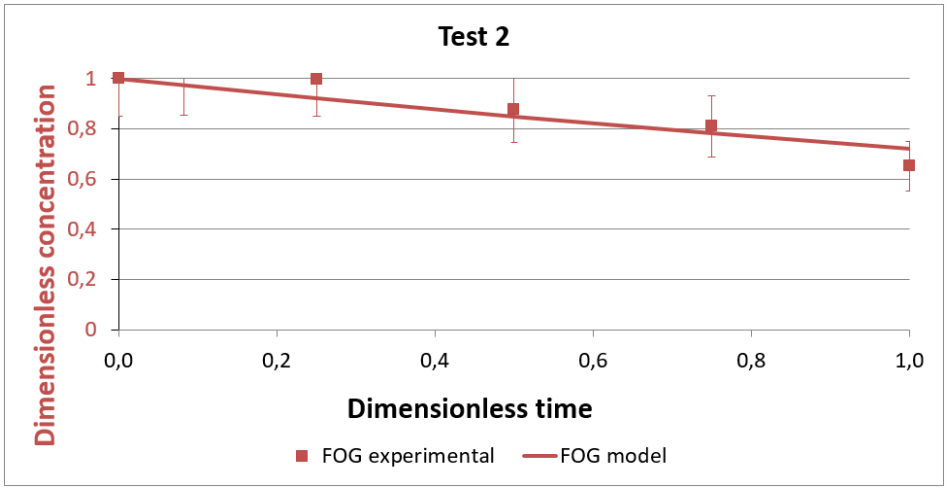

Figure 36. Simulation result of mass transfer of test number 2, continuous and mass transfer coefficient estimated based on test number 2.

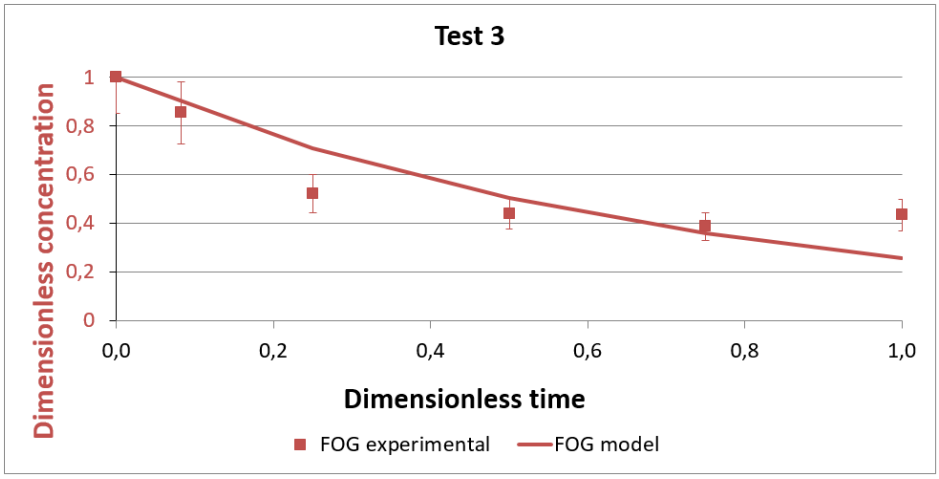

Figure 37. Simulation result of mass transfer of test number 3, continuous and mass transfer coefficient estimated based on test number 3.